European Journal of Medicinal Chemistry 46 (2011) 4419–4429

Contents lists available at ScienceDirect

European Journal of Medicinal Chemistry

journal homepage: http://www.elsevier.com/locate/ejmech

Original article

Design of benzimidazole- and benzoxazole-2-thione derivatives as inhibitors of bacterial hyaluronan lyase

Stephan Braun, Alexander Botzki, Sunnhild Salmen, Christian Textor, Günther Bernhardt, Stefan Dove*, Armin Buschauer

Institute of Pharmacy, University of Regensburg, D-93040 Regensburg, Germany

ARTICLE INFO

Article history:
Received 21 March 2011
Received in revised form
29 June 2011
Accepted 8 July 2011
Available online 19 July 2011

Keywords:
Hyaluronan lyase inhibitors
Streptococcus agalactiae
Structure-based design
Benzimidazole-2-thiones
Benzoxazole-2-thiones

ABSTRACT

Bacterial hyaluronan lyases (Hyal) degrade hyaluronan, an important component of the extracellular matrix, and are involved in microbial spread. Hyal inhibitors may serve as tools to study the role of the enzyme, its substrates and products in the course of bacterial infections. Moreover, such enzyme inhibitors are potential candidates for antibacterial combination therapy. Based on crystal structures of *Streptococcus pneumoniae* Hyal in complex with a hexasaccharide substrate and with different inhibitors, 1-acylated benzimidazole-2-thiones and benzoxazole-2-thiones were derived as new leads for the inhibition of *Streptococcus agalactiae* strain 4755 Hyal. Structure-based optimization led to *N*-(3-phenylpropionyl)benzoxazole-2-thione, one of the most potent compounds known to date (IC_{50} values: 24 μM at pH 7.4, 15 μM at pH 5). Among the 27 new derivatives, other N-acylated benzimidazoles and benzoxazoles are just as active at pH 7.4, but not at pH 5. The results support a binding mode characterized by interactions with residues in the catalytic site and with a hydrophobic patch.

1. Introduction

Hyaluronan, the polyanionic form of hyaluronic acid (HA), is a linear polyglycosaminoglycan consisting of repeating disaccharide units of (β-1,4)-D-glucuronic acid (β-1,3)-*N*-acetyl-D-glucosamine. It was first isolated from the vitreous humor of bovine eyes [1] and is a major component of the extracellular matrix (ECM) of animal tissues. HA is present in the capsule of some bacteria and in essentially all vertebrates where it mainly occurs in the skin and in the CNS [2]. HA interacts with various receptors (e.g., CD44) and hyaluronan binding proteins (hyaladherins like aggrecan, versican, neurocan and brevican) on the surface of cells [3,4]. As main structural element in the matrix HA plays an important role for tissue architecture. Moreover, HA is involved in many biological processes including fertilization, embryonic development, cell migration and differentiation, wound healing, inflammation as well as growth and metastasis of tumor cells [2,4,5].

HA is degraded by hyaluronidases, a class of enzymes with two main families, the eukaryotic hyaluronoglucosaminidases (EC 3.2.1.35) and the prokaryotic hyaluronan lyases (EC 4.2.2.1) [6,7]. The bacterial enzymes cleave HA at the β-1,4-glycosidic linkage between D-glucuronic acid and *N*-acetyl-D-glucosamine. The product of this elimination reaction is the unsaturated disaccharide 2-acetamido-2-deoxy-3-*O*-(β-D-gluco-4-enepyranosyluronic acid)-D-glucose [6,8]. The best characterized hyaluronan lyases are from *Streptococcus pneumoniae* (*Spn*Hyal) and *Streptococcus agalactiae* (*Sag*Hyal) [9,10]. The 3D structures of both enzymes were elucidated by X-ray analyses in the native form as well as in complex with substrates, products and in the case of *Spn*Hyal also with inhibitors [9–16]. Fig. 1 presents an overview of the *Spn*Hyal structure complexed with a hexasaccharide substrate. It consists of an α-helical and a β-sheet domain, both linked by a loop of 10 amino acids. The active site is located in a long cleft and comprises four main parts: a positive patch, a catalytic triad (Asn^{349}, His^{399} and Tyr^{408}) responsible for degradation, a hydrophobic/aromatic patch (Trp^{291}, Trp^{292} and Phe^{343}) responsible for correct positioning of the substrate chains, and a negative patch implicated in the release of the product (Glu^{388}, Asp^{398}, and Thr^{400}) [12].

The *S. pneumoniae* enzyme shows 53% sequence identity with the nearly (98%) identical hyaluronan lyases from two *S. agalactiae* strains, 4755 ($SagHyal_{4755}$) and 3502 ($SagHyal_{3502}$) [17]. However, the amino acids of the active sites of the three enzymes are entirely the same. In contrast to the structure of *Spn*Hyal, a fully active two-

Abbreviations: BSA, bovine serum albumin; CTAB, cetyltrimethylammonium bromide; DMAP, 4-(dimethylamino)pyridine; DMF, dimethylformamide; DMSO, dimethyl sulfoxide; ECM, extracellular matrix; HA, hyaluronan; Hyal, hyaluronan lyase; $SagHyal_{4755}$, *Streptococcus agalactiae* strain 4755 hyaluronan lyase; *Spn*Hyal, *Streptococcus pneumoniae* hyaluronan lyase; TCDI, 1,1′-thiocarbonyl diimidazole; THF, tetrahydrofuran; Vc, L-ascorbic acid; Vcpal, L-ascorbic acid-6-hexadecanoate.

* Corresponding author. Tel.: +49 941 943 4673; fax: +49 941 943 4820.
E-mail address: Stefan.Dove@chemie.uni-regensburg.de (S. Dove).

0223-5234/$ – see front matter © 2011 Elsevier Masson SAS. All rights reserved.
doi:10.1016/j.ejmech.2011.07.014

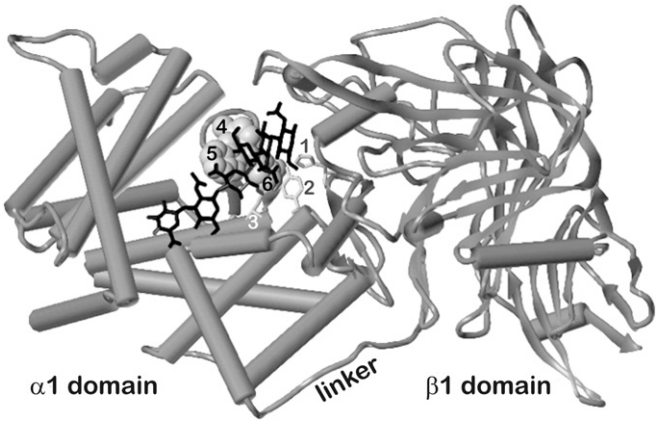

Fig. 1. Schematic representation of the *Spn*Hyal structure in complex with a hexasaccharide substrate (black sticks). Cylinders - α-helices, ribbons - β-sheets. Amino acids of the catalytic triad (**1** – His^{399}, **2** – Tyr^{408}, **3** – Asn^{349}) are shown as graysticks, residues of the hydrophobic patch (**4** – Trp^{291}, **5** – Trp^{292}, **6** – Phe^{343}) as space fill model.

domain truncated version [12], the *Sag*$Hyal_{3502}$ X-ray structure reveals an additional β-sheet domain at the N-terminus and is not catalytically active because of an ~7.3 Å wider binding cleft [13].

HA degradation by hyaluronan lyases consistently results in unsaturated disaccharides, which can be utilized by bacteria as an additional carbon source [18], and leads to reduced viscoelasticity of the ground substance in the ECM of the host. Thus, the spread of the pathogens and of their associated toxins into tissues may be facilitated [18]. Streptococcal hyaluronan lyases can therefore be regarded as significant virulence factors involved in human infections which are major causes of meningitis, pneumonia, septicemia, as well as many other serious diseases that lead to neonatal mortality. Hyaluronan lyase inhibitors may serve as useful pharmacological tools to study the precise role of the enzyme, its substrates and products in the course of bacterial infection and spread and are of potential interest as candidates for antibacterial treatment in combination with antibiotics. However, the detection and the design of inhibitors are still at the beginning (for recent review, see [19]).

Various unsaturated fatty acids inhibited the enzyme from *Streptococcus dysgalactiae* with IC_{50} values ranging from 17 to 172 μM [20]. Glycyrrhetinic acid, a triterpene, was active against *Sag*Hyal (IC_{50} 60 μM) [21]. L-Ascorbic acid (Vc, **1**, Fig. 2) was described as another, but weak competitive inhibitor (IC_{50} ~6 mM) [14]. The crystal structure of the *Spn*Hyal-Vc complex [14] indicated that Vc binds in the active site of the enzyme and that hydrophobic

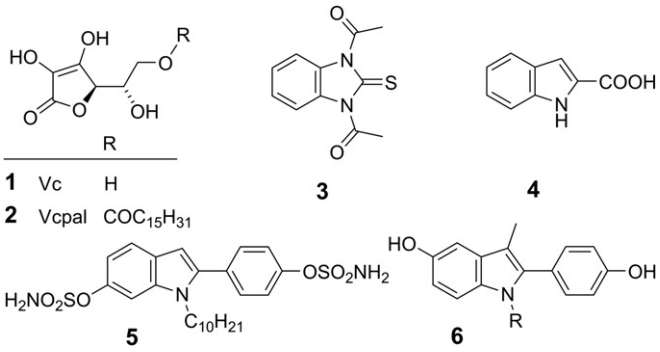

Fig. 2. Chemical structures of hyaluronan lyase inhibitors. **1**: Vitamin C, L-ascorbic acid, Vc; **2**: L-ascorbic acid-6-hexadecanoate, Vcpal; **3**: 1,3-diacetylbenzimidazole-2-thione; **4**: indole-2-carboxylic acid; **5**: 1-decyl-2-(4-sulfamoyloxyphenyl)-1*H*-indol-6-yl sulfamate, **6**: N-substituted 2-(4-hydroxyphenyl)-3-methyl-5-hydroxyindoles.

contacts with Trp^{292} and Tyr^{408} are important. Higher activity was predicted for derivatives which additionally fit to the hydrophobic patch. Indeed, L-ascorbic acid-6-hexadecanoate (Vc palmitate, Vcpal, **2**, Fig. 2), a highly effective antioxidant [22] and glutathione-S-transferase inhibitor [23], showed an IC_{50} value of 4.2 μM at *Sag*$Hyal_{4755}$ [15]. The X-ray structure of the *Spn*Hyal–Vcpal complex [15], determined at 1.65 Å resolution, confirmed the hypothesis that additional hydrophobic interactions with Phe^{343}, His^{399} and Thr^{400} lead to increased inhibition. Within a congeneric series of 6-O-acylated Vc derivatives, L-ascorbic acid-6-octadecanoate was the most potent *Sag*$Hyal_{4755}$ inhibitor (IC_{50} 0.9 μM) [24].

Recent work on hyaluronan lyase inhibitors in our laboratory was focused on the generation of new leads. The program LUDI [25] identified numerous hits by docking of molecules from databases into a *Sag*$Hyal_{4755}$ model [26]. 13 of 19 synthesized compounds proved to be active against *Sag*$Hyal_{4755}$. 1,3-Diacetylbenzimidazole-2-thione (**3**, Fig. 2) was the most potent inhibitor (IC_{50} 5 μM at pH 7.4). Another hit from these investigations, indole-2-carboxylic acid (**4**, Fig. 2), was active only at concentrations above 1 mM, but initiated the rational design of a series of inhibitors based on the 2-phenylindole scaffold [27,28]. The most active compound, 1-decyl-2-(4-sulfamoyloxyphenyl)-1*H*-indol-6-yl sulfamate (**5**, Fig. 2, IC_{50} on *Sag*$Hyal_{4755}$ 11 μM at pH 5, 16 μM at pH 7.4) was crystallized in complex with *Spn*Hyal [16], indicating a similar interaction pattern as in the case of Vcpal. In particular, hydrophobic chains at the indole nitrogen were shown to mimic the hexadecanoyl moiety of Vcpal.

The present study is dealing with the derivation and optimization of two other leads, namely benzimidazole- and benzoxazole-2-thiones, based on comparison of *Spn*Hyal-inhibitor complexes and exploration of possible interaction sites. The synthesis and the structure–activity relationships of these novel *Sag*$Hyal_{4755}$ inhibitors will be described and discussed in the light of a common binding mechanism.

2. Results and discussion

2.1. Lead generation

4-(3-Phenyl-1*H*-indol-2-yl)phenol inhibited bovine testes hyaluronidase (IC_{50} 107 μM) [29]. Based on indole-2-carboxylic acid (**4**, Fig. 2), a hit from structure-based LUDI searches [26], a series of 2-phenylindole derivatives was synthesized and tested for inhibition of *Sag*$Hyal_{4755}$ [27] (to be published elsewhere). For minimum activity, hydroxy, methoxy or ester groups in 5- or 6-position of the indole nucleus and in 4-position of the phenyl ring seem to be necessary. The binding mechanism of 2-phenylindoles could be analyzed by the crystal structure of *Spn*Hyal in complex with 1-decyl-2-(4-sulfamoyloxyphenyl)-1*H*-indol-6-yl sulfamate (**5**, Fig. 2) [16]. Fig. 3 shows that the inhibitor **5** binds in the cleft formed by the α-domain in the area of the catalytic triad (Asn^{349}, His^{399} and Tyr^{408}) and the hydrophobic patch (Trp^{291}, Trp^{292} and Phe^{343}) and, therefore, in the same site in which the HA disaccharide product [17], Vc [14] as well as Vcpal [15] were located in our earlier studies. Hydrophobic interactions of the rings and the aliphatic tail as well as hydrogen bonds of the 6-sulfamoyloxy group contribute to the binding affinity. The indole plane of the inhibitor is in parallel with that of Trp^{292}. The opposite side of the indole moiety interacts with the guanidino group of Arg^{462}. The phenyl nucleus of the inhibitor is sandwiched between Trp^{291} (nearly perpendicular ring arrangement) and Asn^{580}. The decyl chain fits into a surface crevice lined mainly by hydrophobic residues – Trp^{291}, Phe^{343}, Met^{579} – but also by Arg^{336}, Glu^{388} and His^{399}. The 6-sulfamoyloxy group forms a network of hydrogen

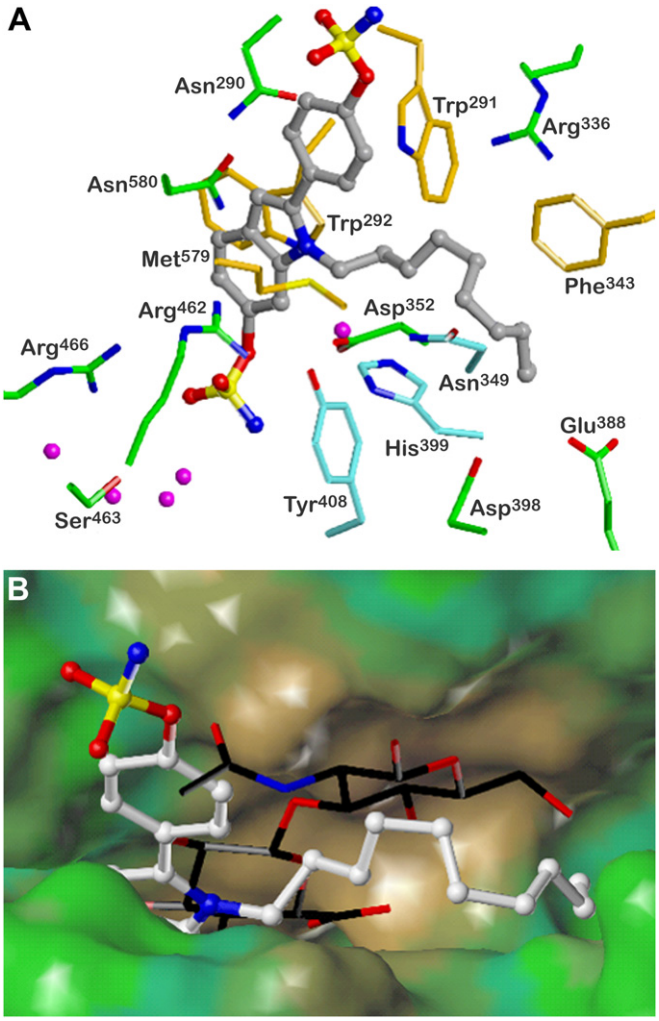

Fig. 3. *Spn*Hyal binding site of the phenylindole inhibitor **5** (view into the substrate binding cleft with the α-domain in the foreground). A) Detailed representation of interactions. Colors of C atoms: inhibitor gray, residues with hydrophobic contacts to the inhibitor orange, catalytic triad cyan, other residues green. Magenta balls: oxygen of water molecules participating in the *Spn*Hyal-inhibitor H-bond network. B) Lipophilic potential of the binding site mapped onto a MOLCAD surface. Cpd. **5** (C atoms white) and a hexasaccharide substrate (C atoms black) are aligned according to a backbone rms fit of the complexes PDB 2BRP and 1LOH. Hydrophobic regions are colored in brown, polar regions in green and green-blue. The 4-sulfamoyloxy substituent is exposed to the solvent. (For interpretation of the references to colour in this figure legend, the reader is referred to the web version of this article.)

bonds with the protein and water, including charge assisted bidentate H bonds between Arg^{466} and two sulfamoyl oxygen atoms. Both oxygen atoms and the nitrogen are additionally linked to the protein by through-water interactions.

In a homologous series of N-substituted 2-(4′-hydroxyphenyl)-3-methyl-5-hydroxyindoles (**6**, Fig. 2), *Sag*$Hyal_{4755}$ inhibition at pH 7.4 increases in the order R = H (IC_{50} 280 μM), methyl (IC_{50} 220 μM), *n*-propyl (IC_{50} 160 μM), *n*-pentyl (IC_{50} 36 μM), and *n*-heptyl (IC_{50} 12 μM) [27]. Thus, the fit of the aliphatic chains to the hydrophobic *Sag*$Hyal_{4755}$ pocket corresponding to *Spn*Hyal Trp^{291}, Phe^{343} and Met^{579} significantly contributes to the binding affinity.

An appropriate strategy to derive new leads from the phenylindole inhibitors is to retain a bicyclic scaffold. The high activity of 1,3-diacetylbenzimidazole-2-thione (**3**, Fig. 2), a hit from LUDI searches [26], provides first clues to possible variations. The benzimidazole moiety may be docked into *Spn*Hyal in superposition with the indole scaffold of compound **5**. This docking mode implies that an unsubstituted nitrogen in 3-position may form a hydrogen bond with the amide oxygen of Asn^{290} (cf. Fig. 3A). Replacing this nitrogen by oxygen leads to benzoxazole-2-thiones. In this case, a hydrogen bond of the benzoxazole oxygen with the amide group of Asn^{290} may be suggested. The acetylation of the N1 nitrogen in compound **5** could enable additional interactions with His^{399}, Tyr^{408} and/or Arg^{462}. Fig. 3B shows the lipophilic potential mapped on the surface of the binding site of *Spn*Hyal together with the phenylindole **5** and a hexasaccharide substrate, both extracted from the respective aligned crystal structures [11,16]. A continuous hydrophobic region ranges from Trp^{292} outwards to Phe^{343}, accommodating parts of the indole ring and nearly the complete decyl chain as well as the HA disaccharide unit to be released. Based on this comparison, the idea was to mimic the terminal *N*-acetylglucosamine moiety by an aromatic or alicyclic ring, i.e., to replace 1-alkanoyl or 1-alkyl substituents by, e.g., ω-phenylalkanoyl groups. 3-Phenyl substituted 1-propionyl derivatives were predicted to be optimal because of possible overlap of the *N*-acetylglucosamine residue with the terminal phenyl moiety.

Fig. 3B indicates that parts of the phenyl moiety and the 4′-substituent project into the solvent. Therefore, shorter groups may be more appropriate. Benzimidazole-2-thiones and benzoxazole-2-thiones are new leads bearing a sulfur atom instead of the 4′-substituted phenyl ring present in compounds **5** and **6**.

2.2. Chemistry

The benzimidazole-2-thione derivatives were synthesized as shown in Fig. 4. The preparation of 1-acetyl-benzimidazole-2-thione (**10**) was performed according to the procedure described by Saxena et al. [30], whereas the other 1-monoacylated benzimidazol-2-thione derivatives **11**–**15** were accessible by a slightly modified protocol using benzimidazol-2-thione **7** as starting material and acid chlorides or acid anhydrides as acylating reagents. Pyridine was used as solvent and base.

1,3-Diacetyl-benzimidazol-2-thione (**3**) was obtained by acetylation of benzimidazole-2-thione with acetyl chloride in the presence of triethylamine as base and *N*,*N*-dimethylaminopyridine (DMAP) as catalyst at room temperature. The 1-hexanoyl homolog **18** was synthesized by treating **13** with acetyl chloride and triethylamine in dry THF (modified protocol according to [31]).

The oxo analog of compound **3**, 1,3-diacetyl-benzimidazol-2-one (**16**), was prepared according to previously described methods [32,33]. From the chemical point of view, **16** is an interesting reagent, but probably, its use as an enzyme inhibitor is limited due to its high reactivity toward nucleophiles, although it is more stable than the corresponding thio analogs.

The alkylated derivatives **9** and **17** were synthesized by modification of published methods [31,34] *via* *N*,*N*′-dialkylation of *o*-phenylenediamine followed by ring closure to obtain the corresponding benzimidazol-2-thiones. *o*-Phenylenediamine was alkylated with bromoethane and sodium hydride as base in DMF yielding both the diethylated (21%) and the monoethylated

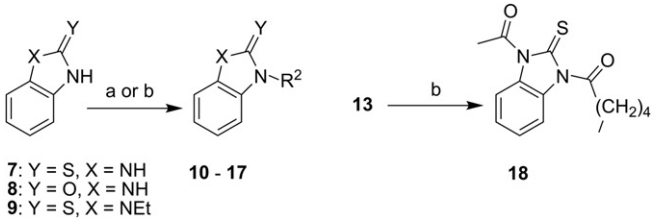

Fig. 4. Synthesis of *N*-mono and diacylated benzimidazole-2-(thi)ones. Reagents and conditions: (a) R^2Cl or $(R^2)_2O$, pyridine (not used for **16**); (b) R^2Cl, Et_3N, THF.

substance (38%). The cyclization was performed with TCDI in anhydrous THF. Overnight stirring at ambient temperature resulted in high yields of **9** (93%) which was converted to **17** by acylation with acetyl chloride in anhydrous THF in the presence of triethylamine.

The preparation of the *N*-acylated benzoxazole-2-(thi)ones **22**–**36** was performed using modified protocols (**22**–**34** [35], **35** and **36** [31]) by treating benzoxazole-2-thiol (**19**) and benzoxazol-2-one (**20**), respectively, with either appropriate acid chloride or acid anhydride in anhydrous THF as shown in Fig. 5. The *N*-alkylated benzoxazole-2-thione **38** was obtained *via* a ring closing reaction of 2-(ethylamino)phenol (**37**) with TCDI (synthesis modified according to [36]).

2.3. Structure–activity relationships

The inhibitory activities (IC_{50} values) of the benzimidazole and benzoxazole derivatives determined by a turbidimetric assay [37] on *Sag*Hyal$_{4755}$ at pH 5.0, the pH optimum of the enzyme, and pH 7.4 are reported in Table 1. Strikingly, all compounds except **28** are more potent at pH 7.4 than at pH 5. It is unlikely that this behavior is simply due to the effect of K_m on the relationship between IC_{50} and K_i since the HA concentrations used in the assays were not significantly greater than estimated K_m values and since the 2-phenylindole **5** and some of its derivatives are equiactive at both pH values, too [27].

Generally the displacement of the thione sulfur by oxygen (**16**, **35**, **36**) leads to inactivity. Further common considerations are that the potencies of the benzimidazoles at pH 5 are much lower than those of the benzoxazoles, and that at least one *N*-acyl substituent must be present since the unsubstituted compounds **7** and **19** as well as the *N*-ethyl derivatives **9** and **38** are nearly inactive in contrast to the 1-acetyl-3-ethyl benzimidazole **17** (IC_{50} 19 μM at pH 7.4).

The diacylated benzimidazole-2-thiones **3** and **18** show the highest inhibitory potency of the whole series at pH 7.4. At pH 5 they are still moderately active in contrast to the almost inactive monoacylated derivatives **10**–**15**. At pH 7.4, the IC_{50} values of **10**–**15** approach those of **3** and **18**, but there is no distinct effect of the chain length since all homologs except the *m*-Cl substituted benzoylated compound **15** are nearly equiactive. This result was rather disappointing with regard to the original intention to fit the acyl chains to the hydrophobic patch like in the case of Vcpal (**2**) and the phenylindole **5**.

By contrast, the SAR of the acylated benzoxazole-2-thiones **22**–**33** are more pronounced. At pH 7.4, the higher open-chained homologs **24**–**26** are by a factor of ~2 more active than the acetyl and propionyl derivatives **22** and **23**, respectively. With a terminal phenyl moiety, optimal potency was observed on 3-phenylpropionyl (**28**) and 4-phenylbutanoyl (**29**) substitution. Having in mind that only compound **28** inhibits *Sag*Hyal$_{4755}$ also at pH 5 with an IC_{50} value in the range of the best results at pH 7.4 (15 μM), it may be concluded that the predicted optimum of the 3-phenylpropionyl group for fit to the hydrophobic patch is confirmed in the case of benzoxazole-2-thiones. Retaining the chain length of **28**, a terminal cyclohexyl moiety (**31**) is still favorable, whereas a phenoxyacetyl group (**32**) reduces the potency by a factor of 3. A benzyloxycarbonyl substituent (**33**) and even more the rigidisation of the chain by introduction of a double bond (**30**) drastically decreases activity.

An additional methoxycarbonyl substituent in 5-position of the benzoxazole ring does not increase *Sag*Hyal$_{4755}$ inhibition (cf. cpd. **19** with **21** and **28** with **34**). Compared to **28**, the activity of cpd. **34** at pH 5 is even more than one order of magnitude lower.

All of the compounds in Table 1 were inactive as inhibitors of bovine testicular hyaluronidase at the highest concentration tested at pH 5.

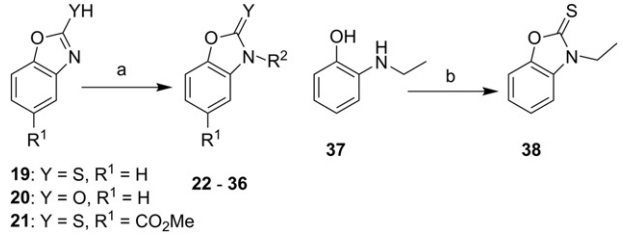

Fig. 5. Synthesis of N-substituted benzoxazole-2-(thi)ones. Reagents and conditions: (a) R^2Cl or $(R^2)_2O$, Et_3N, THF; (b) TCDI, THF.

Table 1
Inhibitory activities (IC_{50} values) of benzimidazole and benzoxazole derivatives determined on *Sag*Hyal$_{4755}$ at pH 5.0 and pH 7.4.

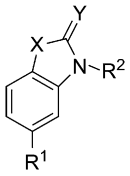

Compound	R^1	R^2	X	Y	hylB$_{4755}$, IC_{50} [μM] or %[a]	
					pH 5.0	pH 7.4
3[b]	H	$COCH_3$	$NCOCH_3$	S	160	5
16[b]	H	$COCH_3$	$NCOCH_3$	O	Inact. (200)	10% (200)
17[b]	H	CH_2CH_3	$NCOCH_3$	S	10% (380)	19 ± 1
18	H	$CO(CH_2)_4CH_3$	$NCOCH_3$	S	50% (49)	12 ± 1
7[b]	H	H	NH	S	1148 ± 50	1862 ± 117
9[b]	H	CH_2CH_3	NH	S	19% (4200)	28% (4200)
10[b]	H	$COCH_3$	NH	S	20% (460)	17 ± 1
11[b]	H	$COCH_2CH_3$	NH	S	4% (180)	26 ± 3
12	H	$CO(CH_2)_2CH_3$	NH	S	7% (190)	20 ± 2
13	H	$CO(CH_2)_4CH_3$	NH	S	14% (170)	16 ± 1
14	H	$CO(CH_2)_2Ph$	NH	S	5% (100)	29 ± 5
15	H	CO-*m*-ClC_6H_4	NH	S	16% (400)	70 ± 10
19[b]	H	H	O	S	42% (3800)	2542 ± 125
21[b]	CO_2CH_3	H	O	S	1299 ± 223	27% (2000)
22[b]	H	$COCH_3$	O	S	125 ± 5	42 ± 3
23[b]	H	$COCH_2CH_3$	O	S	128 ± 5	48 ± 2
24	H	$CO(CH_2)_4CH_3$	O	S	51% (130)	29 ± 1
25	H	$CO(CH_2)_8CH_3$	O	S	41% (100)	25 ± 4
26	H	$CO(CH_2)_{14}CH_3$	O	S	23% (63)	17 ± 1
27	H	$COCH_2Ph$	O	S	260 ± 41	69 ± 2
28[b]	H	$CO(CH_2)_2Ph$	O	S	15 ± 1	24 ± 1
29[b]	H	$CO(CH_2)_3Ph$	O	S	47% (100)	19 ± 1
30[b]	H	COCH=CHPh	O	S	9% (80)	36% (200)
31	H	$CO(CH_2)_2Cy$	O	S	227 ± 122	20 ± 1
32[b]	H	$COCH_2OPh$	O	S	213 ± 30	62 ± 2
33[b]	H	CO_2CH_2Ph	O	S	Inact. (100)	556 ± 20
34	CO_2CH_3	$CO(CH_2)_2Ph$	O	S	56% (200)	21 ± 1
35[b]	H	$COCH_3$	O	O	Inact. (2000)	1466 ± 76
36	H	$CO(CH_2)_4CH_3$	O	O	Inact. (150)	Inact. (300)
38[b]	H	CH_2CH_3	O	S	46% (400)	17% (1000)
Reference compounds[c]						
1 (Vc)					6100 ± 100	
2 (Vcpal)					4.2 ± 0.13	
5					11	16

[a] Inhibition was expressed as IC_{50} ± SEM in μM or as % inhibition at the concentration of inhibitor given in parentheses, highest tested concentrations were dependent on the solubility of the compounds.
[b] The following compounds are not original: **3** [38–40], **7** (purchased), **9** [38], **10** [38,39,41], **11** [39], **16** [33,41], **17** [41], **19** (purchased), **21** [42,43], **22** [35,44], **23** [45], **28** [44,46], **29** [46], **30** [47], **32** [44], **33** [44,48], **35** [31,49], **38** [36,50].
[c] Data of **1** and **2** from Ref. [15], data of **5** from Ref. [16].

2.4. Discussion

The structure–activity relationships of *Sag*Hyal$_{4755}$ inhibition indicate that the predicted binding mode, based on the fit of the bicyclic scaffolds to the indole moiety of the phenylindole **5**, is reasonable at least in the case of the benzoxazole-2-thiones. Fig. 6A shows the most active inhibitor **28** docked into the *Spn*Hyal - compound **5** complex. The benzoxazole oxygen is suggested to form hydrogen bonds with the amide NH_2 groups of Asn^{290} and Asn^{580}. Because of the inactivity of the benzoxazole-2-one compounds **35** and **36**, hydrophobic interactions of the thione sulfur with Trp^{291} and Trp^{292} are predicted. These interactions partially replace those of the 2-phenyl group in compound **5** (see Fig. 3A). The remarkable increase in potency observed for 1-acylated *vs*. 1-alkylated derivatives (compare e.g., cpds. **22** and **38**) suggests that the acyl oxygen contributes to binding. Its short distance (<3Å) to the imidazolyl, hydroxy and guanidino groups of His^{399}, Tyr^{408} and Arg^{462}, respectively, indicates hydrogen bonds and/or ion–dipole interactions (see Fig. 6A). The phenylpropionyl moiety of compound **28** mainly interacts with Trp^{291} and Phe^{343} (hydrophobic patch), but also with Arg^{336} (cation–π interactions) and His^{399}. Because of the similar potency of compounds **5** and **28**, it may be speculated that some interactions of **5**, in particular of the 6-sulfamoyloxy group and of the 2-phenyl substituent, are compensated in the case of acylated benzoxazole-2-thiones by interactions of the acyl function, the oxazole oxygen and the thione sulfur.

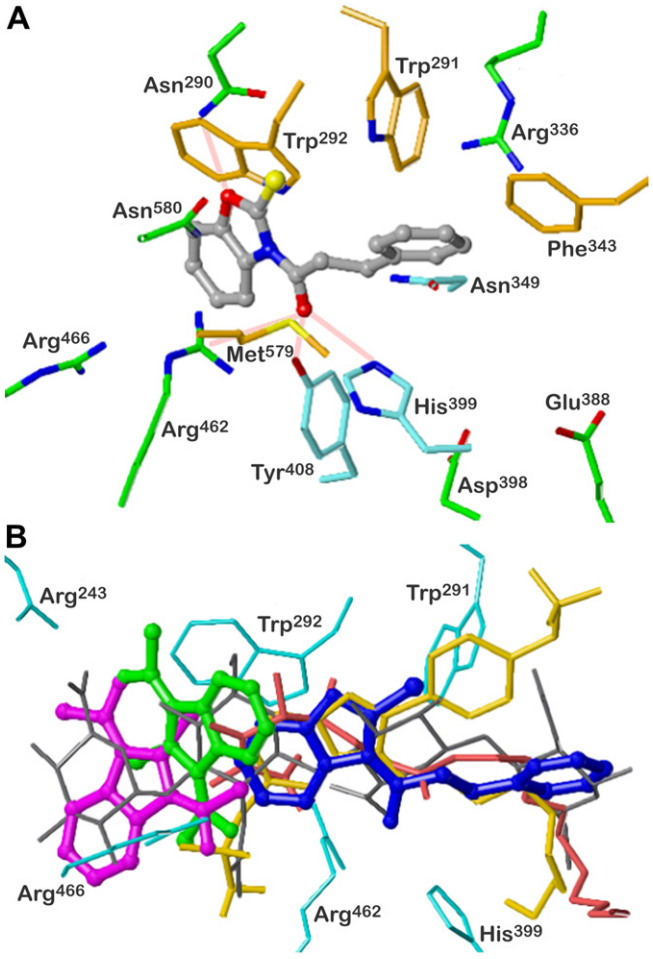

Fig. 6. Putative *Spn*Hyal binding sites of the benzoxazole-2-thione **28** and 1,3-diacetylbenzimidazole-2-thione **3**. (A) Detailed representation of the suggested interactions of cpd. **28**, docked into the crystal structure PDB 2BRP (view corresponding to Fig. 3A). Colors of C atoms: inhibitor gray, residues with hydrophobic contacts to the inhibitor orange, catalytic triad cyan, other residues green. Pink lines: suggested key interactions. (B) Comparison of the putative binding modes of cpds. **28** (blue) and **3** (predicted by LUDI [25] using sphere radii of 5 Å – pose 1, magenta, and 8 Å – pose 2, green) with binding modes of a hexasaccharide substrate (gray, only disaccharide units 1 and 2 around the scissile bond drawn), of Vcpal (**2**, red) and the phenylindole **5** (yellow). The alignment is based on backbone rms fits of the PDB complexes 2BRP (cpd. **5**), 1LOH (hexasaccharide), 1W3Y (Vcpal), and the *Sag*Hyal$_{4755}$ model used for LUDI searches (cpd. **3**). For better orientation, some important *Spn*Hyal residues are shown (cyan). (For interpretation of the references to colour in this figure legend, the reader is referred to the web version of this article.)

In Fig. 6B, the docking pose of compound **28** is compared with the binding modes of a hexasaccharide substrate [11], of Vcpal (**2**) [15] and of the phenylindole **5** [16]. The more or less polar cores and the hydrophobic chains of the inhibitors are largely aligned. The heterocyclic scaffolds of compounds **5** and **28** as well as the ring-opened [15] vitamin C moiety of Vcpal occupy the region around the scissile bond of the substrate, whereas the alkyl or arylalkanoyl chains correspond to the disaccharide unit to be released. Obviously, the 3-phenylpropionyl group of the benzoxazole-2-thione **28** optimally aligns with this HA unit since the 1,3-glycosidic linkage is mimicked by the two methylene groups and since the *N*-acetyl-glucosamine residue overlaps with the terminal phenyl ring.

Fig. 6B additionally contains the binding modes predicted for 1,3-diacetylbenzimidazole-2-thione (**3**). Using a *Sag*Hyal$_{4755}$ model, two possible poses resulted from LUDI runs [25] with different search spheres (radii of 5 and 8 Å, respectively) [26]. The two poses adopt nearly mirror-inverted positions. In each pose, the acetyl groups interact with the guanidine moieties of two arginines (*Spn*Hyal: Arg^{243} and Arg^{466}) bridging the walls at the narrowest site of the HA binding cleft, and the thione sulfur is less than 3.5 Å distant from a Trp side chain corresponding to *Spn*Hyal Trp^{292}. However, the predicted poses are rather questionable in the light of the SAR. The high activity of the hexanoyl derivative **18** is still conceivable since the alkanoyl chain might align with the long HA binding cleft on both sides, and also the lower potency of the 1-ethyl-substituted benzimidazole **17** is not surprising due to the presence of only one acetyl group. But there is no reasonable explanation for the inactivity of the benzimidazole-2-one **16**. It may be speculated that the binding mode of compound **3** corresponds to that of the phenylindole **5**, but a close superposition of both heterocyclic scaffolds on docking to the *Spn*Hyal structure is impossible because of steric clashes of one of the acetyl groups with Asn^{290} and Asn^{580}. However, considering the specific topology of the substrate binding site – a rather long cleft instead of a deep pocket like in many other enzymes – multiple and overlapping inhibitor binding modes may exist, especially in the case of small molecules like **3**.

The binding mode of the benzimidazole-2-thiones **10**–**15** may be similar to that of the benzoxazole-2-thiones **22**–**33**. The NH function in 3-position, however, suggests interaction with the amide oxygens of Asn^{290} and/or Asn^{580}. The temperature factors of the ligand-free *Spn*Hyal structure [12] indicate high flexibility of the Asn^{290} side chain unlike that of Asn^{580}. As a consequence, the benzimidazole-2-thiones may dock in a position which slightly differs from the binding modes in Fig. 3A and Fig. 6A and which is characterized by the same type of interactions as in the case of the benzoxazole derivatives. This would explain why the optimal members of both series are equipotent at pH 7.4 and why both N^1-ethylated compounds **9** and **38** are inactive, but also why the effects of the chain lengths are different.

According to the binding mode of the phenylindole **5** (see Figs. 3 and 6B), an additional methoxycarbonyl substituent in 5-position of the benzoxazole ring should actually improve *Sag*Hyal$_{4755}$ inhibition since in the model in Fig. 6 the oxygen atoms of this polar group would fit to appropriate amino acids (Tyr^{408}, Arg^{462}, Arg^{466})

like the corresponding 6-sulfamoyloxy group of compound **5**. However, no increase in potency was observed for compounds **21** and **34**. Possible reasons are slight differences between the *Sag*Hyal$_{4755}$ and *Spn*Hyal binding sites or a nearly unchanged free energy balance if H bonds are replaced by through-water interactions.

The pH influence on the inhibitory activity is difficult to interpret. Generally greater IC_{50} values of the inhibitors at the pH optimum of 5 could be due to higher affinity of the substrate HA. However, a number of *Sag*Hyal$_{4755}$ inhibitors (e.g., **28**, some phenylindoles [27] and LUDI hits [26]) prefer pH 5. Therefore the protonation state of some active site residues (glutamates, aspartates and the histidine of the catalytic triad) may directly affect the binding of individual compounds. But why are just benzimidazole-2-thiones inactive at pH 5? It is surely too simple to explain this result by the different states of a single amino acid like the histidine corresponding to *Spn*Hyal His^{599}. The analysis of two new *Spn*Hyal structures revealed the great flexibility of the substrate binding site, allowing open and closed conformations of the cleft and, by this, the controlled sequence of HA binding, catalysis, disaccharide release and translocation of the substrate by one disaccharide unit to the next cleavage position [51]. The influence of the flexibility and the different conformations on inhibitor association and dissociation is hardly to interpret, all the more as all *Spn*Hyal structures were analyzed at pH 6–6.5 (close to the optimum of this enzyme). The lower pH optimum of *Sag*Hyal$_{4755}$ may point to slightly different energetic and conformational properties which are not sufficiently reflected by flexible docking of the inhibitors to *Spn*Hyal.

Also the 5- to 25-fold reduced inhibitory potency of Vc, Vcpal and the phenylindole **5** at *Spn*Hyal compared to *Sag*Hyal$_{4755}$ [16] indicates that both enzymes with identical active site residues differ in conformational details. Since the V_{max} values are similar and since a reduction of the HA concentration did not significantly lower IC_{50}, the weaker *Spn*Hyal activity should be attributed to the inhibitors themselves, e.g., to slower association or higher dissociation rates due to the specific topology around the binding cleft or to the flexibility of the enzyme–inhibitor complexes.

3. Conclusions

Based on crystal structures of *Spn*Hyal–ligand complexes with a hexasaccharide substrate and with the inhibitors **2** and **5**, respectively, 1-acylated benzimidazole-2-thiones and benzoxazole-2-thiones were derived as new leads for the inhibition of streptococcal hyaluronan lyases. In the benzoxazole series, structure-based optimization of the 1-substituents led to *N*-(3-phenylpropionyl)benzoxazole-2-thione (**28**) with IC_{50} values of 24 μM (pH 7.4) and 15 μM (pH 5) on *Sag*Hyal$_{4755}$. The high potency of **28** at the pH optimum (pH 5) is unique among all analyzed derivatives; this compound is among the three most potent *Sag*Hyal$_{4755}$ inhibitors known so far (IC_{50} values at pH 5 for Vcpal 4.2 μM, for the phenylindole **5** 11 μM). At physiological pH also some other benzimidazole-2-thione and benzoxazole-2-thione derivatives like **17**, **18**, **10**–**14**, **24**–**26**, **29** and **31**, respectively, inhibit *Sag*Hyal$_{4755}$ with potencies close to that of the most active compound **3**. Especially in the case of the benzoxazoles, the structure–activity relationships are in agreement with the proposed binding mode characterized by polar interactions of the oxazole and the acyl oxygens with asparagine, arginine, tyrosine and histidine residues in the active site and by fitting of the thione sulfur and the alkanoyl or arylalkanoyl chain to the hydrophobic patch of the enzyme. The results provide a basis for further structure-based inhibitor design to optimize potency, selectivity and pharmacokinetic properties. Additional investigations toward antibacterial properties *in vivo* are intended, since inhibition of the spreading of pathogenic *Streptococci* in such infections as bacteremia and meningitis may reduce or even avoid the application of classical antibiotics.

4. Experimental protocols

4.1. Chemical syntheses

Starting materials and solvents were purchased from Acros Organics (Belgium), Lancaster Synthesis GmbH (Germany), Sigma–Aldrich Chemie GmbH (Germany) or Merck (Germany). THF was distilled from NaH. Commercially available petroleum ether (60–80 °C) was distilled before use and dichloromethane was either dried over $CaCl_2$ or distilled from P_2O_5. All other solvents used were of analytical grade.

Nuclear Magnetic Resonance (^{1}H NMR and ^{13}C NMR) spectra were recorded on a Bruker ARX-300 NMR spectrometer with perdeuterated dimethyl sulfoxide (DMSO-d_6) or deuterated chloroform ($CDCl_3$). The chemical shift δ is given in parts per million (ppm) with reference to the chemical shift of the residual protic solvent compared to tetramethylsilane (TMS, $\delta = 0$ ppm). Coupling constants (J) are reported in Hz throughout. 2D-NMR (H–H and C–H) COSY techniques were used in a few cases to support interpretation of 1D spectra. Mass spectrometry analysis (MS) was performed on a Finnigan MAT 95 (PI-EIMS, 70 eV) or a Finnigan SSQ 710A (PI-EIMS, 70 eV, CI-MS (NH_3)) spectrometer. Melting points (Mp) were measured on a BÜCHI 530 electrically heated copper block apparatus using an open capillary and are uncorrected. Column chromatography was carried out using Merck silica gel SI 60 (0.063–0.200). Elemental analyses were performed by the Department of Microanalysis, University of Regensburg. Compounds were dried *in vacuo* (0.1–1 Torr) at room temperature or with heating up to 50 °C for at least 24 h prior to submission for elemental analysis. Analyses indicated by the symbols of the elements or functions were within ±0.4% of the theoretical values. Reactions were routinely monitored by thin layer chromatography (TLC) on Merck silica gel 60 F_{254} aluminum sheets, and spots were visualized with UV light at 254 nm.

4.1.1. 1,3-Diacetylbenzimidazole-2-thione (*3*)

A mixture of benzimidazole-2-thione (**7**) (1.5 g, 10 mmol), triethylamine (2.88 g, 28.5 mmol), a catalytic amount (100 mg) of DMAP and anhydrous dichloromethane was stirred at room temperature for 10 min. A solution of acetyl chloride (2.83 g) and anhydrous dichloromethane was added dropwise and stirring was continued for 16 h. After diluting with water (100 ml) and dichloromethane (50 ml), the organic layer was separated, washed three times with an aqueous solution of potassium hydrogen sulfate (1 M, 50 ml) and water (50 ml) and dried over sodium sulfate. The solvent was removed under reduced pressure, and the product was purified by column chromatography on silica gel eluting with a 1:8 (v/v) mixture containing ethyl acetate and petroleum ether at 60–80 °C to give a white solid. The product decomposes at ambient temperature and moisture to 1-acetylbenzimidazole-2-thione. Yield 1.3 g (5.55 mmol), 56%, white solid. Mp: 100–102 °C (Mp: 102–103 °C [40]). ^{1}H NMR ($CDCl_3$) δ 3.05 (s, 6H, OCH_3), 7.31 (dd, 2H, $^4J = 3.4$ Hz, $^3J = 6.3$ Hz, H-5 and H-6), 7.97 (dd, 2H, $^4J = 3.4$ Hz, $^3J = 6.3$ Hz, H-4 and H-7). MS (EI) m/z 234 ($M^{\bullet+}$). Anal. ($C_{11}H_{10}N_2O_2S$) C, H, N, S.

4.1.2. Synthesis of the monoacylated benzimidazoles *10*–*15*

The following procedures are modifications of the protocol described in Ref. [30].

General method: Benzimidazole-2-thiol (**7**) (1 eq) and pertinent acid chloride or acid anhydride (1.1 eq) were dissolved in pyridine (4.4 eq) under a nitrogen atmosphere. The reaction mixture was stirred overnight at room temperature. After quenching with water (10–25 ml), ethyl acetate (30–45 ml) was added. The organic phase was extracted with 3M hydrochloric acid (3 × 25 ml), dried over magnesium sulfate and concentrated under reduced pressure. The crude product was purified as stated below.

*4.1.2.1. 1-(2-Thioxo-1H-benzo[d]imidazol-1-yl)ethanone (**10**).* Yield: 3.80 g (19.77 mmol, 74%, white solid). Mp: 193–194 °C (Mp: 198–200 °C [30]). ^{1}H NMR (DMSO-d_6): δ 3.00 (s, 3H, CH_3), 7.16–7.33 (m, 3H, Ar–H), 7.97–8.02 (m, 1H, Ar–H), 13.31 (br, 1H, NH). MS (EI): *m/z* (%) 192 ([M•$^+$], 20), 150 ([M − CH_2CO]$^+$, 100). Anal. ($C_9H_8N_2OS$) C, H, N.

*4.1.2.2. 1-(2-Thioxo-1H-benzo[d]imidazol-1-yl)propan-1one (**11**).* Reaction of **7** (1.03 g, 6.86 mmol) with propanoyl chloride (0.64 ml, 7.33 mmol) and pyridine (2.40 ml, 29.73 mmol); recrystallization from ethyl acetate. Yield: 0.78 g (3.79 mmol, 55%, white flakes), Mp: 176–177.5 °C, ^{1}H NMR (DMSO-d_6): δ 1.19 (t, 3H, ^3J = 7.1 Hz, $CH_2\underline{CH_3}$), 3.56 (q, 2H, ^3J = 7.1 Hz, $\underline{CH_2}CH_3$), 7.17–7.34 (m, 3H, Ar–H), 7.97–8.02 (m, 1H, Ar–H), 13.29 (br, 1H, NH). MS (EI): *m/z* (%) 206 ([M•$^+$], 6), 150 ([M − CH_3CHCO]$^+$, 100). Anal. ($C_{10}H_{10}N_2OS$) C, H, N, S.

*4.1.2.3. 1-(2-Thioxo-1H-benzo[d]imidazol-1-yl)butan-1-one (**12**).* Reaction of **7** (1.00 g, 6.66 mmol) with butyric anhydride (1.20 ml, 7.32 mmol) and pyridine (2.40 ml, 29.73 mmol); crude product was treated with a 2:1 (v/v) mixture of petroleum ether (boiling point range 60–80 °C) and ethyl acetate to separate pure product; analytically pure product was obtained by column chromatography on silica gel eluting with a 4:1 (v/v) mixture of petroleum ether (60–80 °C) and ethyl acetate. Yield: 0.98 g (4.45 mmol, 67%, white solid). Mp: 152–153 °C. ^{1}H NMR (DMSO-d_6): δ 0.98 (t, 3H, ^3J = 7.4 Hz, $(CH_2)_2\underline{CH_3}$), 1.67–1.81 (m, 2H, $CH_2\underline{CH_2}CH_3$), 3.56 (t, 2H, ^3J = 7.3 Hz, $COCH_2$–), 7.17–7.34 (m, 3H, Ar–H), 7.95–8.00 (m, 1H, Ar–H), 13.29 (br, 1H, NH). ^{13}C NMR (DMSO-d_6): δ = 13.3 (+, CH_3), 17.6 (−, CH_2), 40.7 (−, CH_2), 109.4 (+, Ar–C), 115.0 (+, Ar–C), 123.3 (+, Ar–C), 125.2 (+, Ar–C), 130.9 (C_{quart}, Ar–C), 131.0 (C_{quart}, Ar–C), 169.4 (C_{quart}, CS), 175.1 (C_{quart}, CO). MS (EI): *m/z* (%) 220 ([M•$^+$], 13), 150 ([M − C_4H_9CHCO]$^+$, 100). Anal. ($C_{11}H_{12}N_2OS$) C, H, N, S.

*4.1.2.4. 1-(2-Thioxo-1H-benzo[d]imidazol-1-yl)hexan-1-one (**13**).* Reaction of **7** (1.02 g, 6.79 mmol) with hexanoic anhydride (1.80 ml, 7.81 mmol) and pyridine (2.40 ml, 29.73 mmol); purification by column chromatography on silica gel, elution with a 4:1 (v/v) mixture of petroleum ether (60–80 °C) and ethyl acetate. Yield: 0.58 g (2.34 mmol, 34%, white solid). Mp: 132.5–133 °C. ^{1}H NMR (DMSO-d_6): δ 0.89 (t, 3H, ^3J = 7.0 Hz, $(CH_2)_4\underline{CH_3}$), 1.28–1.40 (m, 4H, $(\underline{CH_2})_2CH_3$), 1.67–1.78 (m, 2H, $COCH_2\underline{CH_2}$–), 3.57 (t, 2H, ^3J = 7.3 Hz, $\underline{COCH_2}$–), 7.17–7.33 (m, 3H, Ar–H), 7.94–7.99 (m, 1H, Ar–H), 13.29 (br, 1H, NH). ^{13}C NMR (DMSO-d_6): δ 13.7 (+, CH_3), 21.8 (−, CH_2), 23.7 (−, CH_2), 30.5 (−, CH_2), 38.7 (−, CH_2), 109.5 (+, Ar–C), 115.0 (+, Ar–C), 123.3 (+, Ar–C), 125.2 (+, Ar–C), 130.9 (C_{quart}, Ar–C), 131.1 (C_{quart}, Ar–C), 169.4 (C_{quart}, CS), 175.2 (C_{quart}, CO). MS (EI): *m/z* (%) 248 ([M•$^+$], 9), 150 ([M − C_4H_9 − CHCO]$^+$, 100). Anal. ($C_{13}H_{16}N_2OS$) C, H, N, S.

*4.1.2.5. 1-(2-Thioxo-1H-benzo[d]imidazol-1-yl)-3-phenylpropan-1-one (**14**).* Reaction of **7** (0.50 g, 3.33 mmol) with 3-phenylpropanoyl chloride (0.50 ml, 3.33 mmol) and pyridine (2.20 ml, 26.98 mmol); purification with a 5:2 (v/v) mixture of petroleum ether (60–80 °C) and ethyl acetate. Yield: 0.46 g (1.63 mmol, 49%, white solid). Mp: 161–162.5 °C. ^{1}H NMR (DMSO-d_6): δ 3.05 (t, 2H, ^3J = 7.8 Hz, $COCH_2\underline{CH_2}Ph$), 3.90 (t, 2H, ^3J = 7.8 Hz, $COCH_2\underline{CH_2}Ph$), 7.16–7.34 (m, 8H, Ar–H), 7.96–7.99 (m, 1H, Ar–H), 13.33 (br, 1H, NH). ^{13}C NMR (DMSO-d_6): δ 30.0 (−, CH_2), 40.7 (−, CH_2), 109.5 (+, Ar–C), 115.1 (+, Ar–C), 123.3 (+, Ar–C), 125.3 (+, Ar–C), 126.0 (+, Ar–C), 128.3 (+, 4Ar–C), 130.9 (C_{quart}, Ar–C), 131.1 (C_{quart}, Ar–C), 140.5 (C_{quart}, Ar–C), 169.4 (C_{quart}, CS), 174.4 (C_{quart}, CO). MS (EI): *m/z* (%) 282 ([M•$^+$], 6), 249 ([M − SH]$^+$, 19), 150 ([M − $C_6H_5CH_2CHCO$]$^+$, 100), 91 ([C_7H_7]$^+$, 28). Anal. ($C_{16}H_{14}N_2OS$) C, H, N, S.

*4.1.2.6. (3-Chlorophenyl)(2-thioxo-1H-benzo[d]imidazol-1-yl)methanone (**15**).* Reaction of **7** (0.30 g, 2.00 mmol) with *m*-chlorobenzoyl chloride (0.26 ml, 2.00 mmol) and pyridine (3.50 ml, 42.92 mmol); purification by flash column chromatography on silica gel, elution with dichloromethane. Yield: 0.13 g (0.45 mmol, 23%, pale yellow solid). Mp: 170–172 °C. ^{1}H NMR (DMSO-d_6): δ 7.21–7.35 (m, 3H, benzimidazole–H), 7.45–7.48 (m, 1H, benzimidazole–H), 7.55 (ddd, 1H, ^3J = 8.1 Hz, ^3J = 7.7 Hz, ^5J = 0.4 Hz, H-5), 7.75 (ddd, 1H, ^3J = 8.1 Hz, ^4J = 2.1 Hz, ^5J = 1.1 Hz, H-4/6), 7.80 (ddd, 1H, ^3J = 7.7 Hz, ^4J = 1.7 Hz, ^5J = 1.1 Hz, H-4/6), 7.91 (ddd, 1H, ^4J = 2.1 Hz, ^4J = 1.7 Hz, ^5J = 0.4 Hz, H-2), 13.29 (br, 1H, NH). ^{13}C NMR (DMSO-d_6): δ 110.0 (+, Ar–C), 112.1 (+, Ar–C), 123.2 (+, Ar–C), 124.9 (+, Ar–C), 128.8 (+, Ar–C), 129.7 (+, Ar–C), 130.5 (+, Ar–C), 131.3 (C_{quart}, Ar–C), 131.9 (C_{quart}, Ar–C), 133.1 (C_{quart}, Ar–C), 133.5 (+, Ar–C), 134.8 (C_{quart}, Ar–C), 168.5 (C_{quart}, CO), 169.5 (C_{quart}, CS). MS (EI): *m/z* (%) 288 ([M•$^+$], 41), 139 ([ClC_6H_4CO]$^+$, 100), 111 ([ClC_6H_4]$^+$, 47) Anal. ($C_{14}H_9ClN_2OS$) C, H, N, S.

*4.1.3. 1,3-Diacetyl-1H-benzo[d]imidazol-2(3H)-one (**16**)*

The protocol described in Ref. [33] was modified. 2-Hydroxybenzimidazole (**8**) (0.50 g, 3.73 mmol) was suspended in acetic anhydride (15 ml) and heated under reflux for 6 h. Water (20 ml) and ethyl acetate (30 ml) were added and the separated organic phase was extracted with a solution of saturated sodium carbonate (3 × 20 ml). The organic layer was washed with water (20 ml), dried over magnesium sulfate and concentrated under reduced pressure. The crude product was recrystallized from a 1:1 (v/v) mixture of petroleum ether (60–80 °C) and ethyl acetate. Yield: 0.59 g (2.70 mmol, 73%, white needles). Mp: 145.5–146.5 °C (Mp: 149–151 °C [33]). ^{1}H NMR (DMSO-d_6): δ 2.65 (s, 6H, 2$COCH_3$), 7.21–7.37 (m, 2H, Ar–H), 8.03–8.18 (m, 2H, Ar–H). ^{13}C NMR (DMSO-d_6): δ 25.8 (+, 2CH_3), 114.4 (+, 2Ar–C), 124.8 (+, 2Ar–C), 126.5 (C_{quart}, 2Ar–C), 150.6 (C_{quart}, CO), 170.1 (C_{quart}, 2$COCH_3$). MS (EI): *m/z* (%) 218 ([M•$^+$], 15), 176 ([M − CH_2CO]$^+$, 18), 134 ([M − 2CH_2CO]$^+$, 100). Anal. ($C_{11}H_{10}N_2O_3$) C, H, N.

*4.1.4. 1-(3-Ethyl-1,2-dihydro-2-thioxobenzo[d]imidazole-1-yl) ethanone (**17**)*

The protocol described in Ref. [31] was modified. A mixture of 1-ethyl-1*H*-benzo[*d*]imidazole-2(3*H*)-thione (**9**) (0.14 g, 0.79 mmol), dissolved in absolute THF (5 ml), triethylamine (0.11 ml, 0.79 mmol) and acetyl chloride (0.07 ml, 0.98 mmol) was stirred at room temperature for 1 h under an inert atmosphere. The reaction mixture was concentrated under reduced pressure, and water (5 ml) was added. After extraction with ethyl acetate (3 × 10 ml), the combined organic layers were dried over magnesium sulfate and concentrated *in vacuo*. The crude product was purified by column chromatography on silica gel eluting with a 4:1 (v/v) mixture of petroleum ether (60–80 °C) and ethyl acetate. Yield: 0.07 g (0.32 mmol, 40%, white solid). Mp: 81.5–82.5 °C. ^{1}H NMR (DMSO-d_6): δ 1.27 (t, 3H, ^3J = 7.1 Hz, $CH_2\underline{CH_3}$), 3.03 (s, 3H, $COCH_3$), 4.37 (q, 2H, ^3J = 7.1 Hz, $\underline{CH_2}CH_3$), 7.28–7.43 (m, 2H, Ar–H), 7.52–7.57 (m, 1H, Ar–H), 8.03–8.08 (m, 1H, Ar–H). MS (EI): *m/z* (%) 220 ([M•$^+$], 42), 178 ([M − CH_2CO]$^+$, 97), 150 ([M − C_2H_4 − CH_2CO]$^+$, 100), 43 ([H_3C − CO]$^+$, 24). Anal. ($C_{11}H_{12}N_2OS$) C, H, N.

*4.1.5. 1-(3-Acetyl-1,2-dihydro-2-thioxobenzo[d]imidazol-1-yl) hexan-1-one (**18**)*

The protocol described in Ref. [31] was modified. Acetyl chloride (0.10 ml, 1.40 mmol) was added to a mixture of 1-(2-thioxo-1*H*-benzo[*d*]imidazol-1-yl)hexan-1-one (**13**) (0.29 g, 1.17 mmol), triethylamine (0.19 ml, 1.37 mmol) and absolute THF (10 ml). After stirring for 1 h at room temperature, the reaction mixture was concentrated *in vacuo*. Water (10 ml) was added and the aqueous phase was extracted with ethyl acetate (3 × 10 ml). The combined organic layers were washed with a solution of saturated sodium carbonate (10 ml), dried over magnesium sulfate and concentrated under reduced pressure. The crude product was purified by column chromatography on silica gel eluting with an 8:1 (v/v) mixture of petroleum ether (60–80 °C) and ethyl acetate. Yield: 20 mg (0.07 mmol, 6%, white solid). ^{1}H NMR (DMSO-d_6): δ 0.88 (t, 3H, ^3J = 7.1 Hz, $(CH_2)_4\underline{CH_3}$), 1.29–1.40 (m, 4H, $(\underline{CH_2})_2CH_3$), 1.70–1.80 (m, 2H, $COCH_2\underline{CH_2}-$), 2.98 (s, 3H, $COCH_3$), 3.45 (t, 2H, ^3J = 7.3 Hz, $COCH_2-$), 7.34–7.40 (m, 2H, Ar–H), 7.69–7.74 (m, 1H, Ar–H), 7.86–7.90 (m, 1H, Ar–H). Anal. ($C_{15}H_{18}N_2O_2S$) C, H, N.

*4.1.6. 1-Ethyl-1H-benzo[d]imidazole-2(3H)-thione (**9**)*

The protocol described in Ref. [34] was modified. N^1-Ethylbenzene-1,2-diamine (0.23 g, 1.69 mmol) was dissolved in absolute THF (10 ml). This solution was treated with TCDI (0.33 g, 1.85 mmol) under a nitrogen atmosphere. After stirring at room temperature for 22 h, the mixture was concentrated *in vacuo*. Ethyl acetate (15 ml) and water (15 ml) were added to the residue and the organic phase was separated. The aqueous phase was extracted three times with ethyl acetate (15 ml). The combined organic phases were dried over magnesium sulfate and concentrated *in vacuo*. The crude product was purified by column chromatography on silica gel eluting with a 1:1 (v/v) mixture of petroleum ether (60–80 °C) and ethyl acetate. Yield: 0.28 g (1.57 mmol, 93%, white needles). Mp: 161.5–162.5 °C (Mp: 158–161 °C [38]). ^{1}H NMR (DMSO-d_6): δ 1.23 (t, 3H, ^3J = 7.1 Hz, $CH_2\underline{CH_3}$), 4.26 (q, 2H, ^3J = 7.1 Hz, $\underline{CH_2}CH_3$), 7.08–7.28 (m, 3H, Ar–H), 7.31–7.47 (m, 1H, Ar–H), 12.74 (s, 1H, NH). ^{13}C NMR (DMSO-d_6): δ 12.8 (+, CH_3), 37.9 (−, CH_2), 109.3 (+, Ar–C), 109.6 (+, Ar–C), 122.1 (+, Ar–C), 122.7 (+, Ar–C), 130.7 (C_{quart}, Ar–C), 131.9 (C_{quart}, Ar–C), 167.6 (C_{quart}, CS). MS (EI): *m*/*z* (%) 178 ([M$^{\bullet+}$], 100), 150 ([M − C_2H_4]$^+$, 91). Anal.: ($C_9H_{10}N_2S$) C, H, N.

*4.1.7. Synthesis of the benzoxazoles **22**–**34***

The following procedures are modifications of the protocol described in Ref. [35].

Method A. Benzoxazole-2-thiol (**19**) (1 eq) was dissolved in absolute THF (5 ml) under an inert atmosphere. Triethylamine (1.1 eq) was added and the solution was cooled to 0 °C. The particular acid chloride (1 eq), dissolved in 5 ml absolute THF, was added dropwise. After stirring for 30 min at room temperature, the reaction mixture was poured into ice water (35 ml). The precipitated product was collected, washed with water, dried *in vacuo* and recrystallized.

Method B. Benzoxazole-2-thiol (**19**) (1 eq) was dissolved in absolute THF (5 ml) and mixed with triethylamine (1.1 eq) under a nitrogen atmosphere. Alkanoic anhydride (1 eq) was added dropwise and the mixture was heated under reflux (7 h). After diluting with water (30 ml), the mixture was extracted three times with ethyl acetate (10 ml). The combined organic phases were washed with a saturated solution of sodium carbonate (10 ml), dried over magnesium sulfate and the solvent was removed under reduced pressure. The product was purified by column chromatography on silica gel.

*4.1.7.1. 1-(2-Thioxobenzo[d]oxazol-3(2H)-yl)ethanone (**22**). Method A*: Reaction of **19** (0.50 g, 3.31 mmol) with acetyl chloride (0.24 ml, 3.36 mmol); recrystallization from cyclohexane. Yield: 0.46 g (2.38 mmol, 72%, beige solid). Mp: 113–114 °C (Mp: 120–121 °C [35]). ^{1}H NMR (DMSO-d_6): δ 2.94 (s, 3H, $COCH_3$), 7.37–7.44 (m, 2H, Ar–H), 7.55–7.60 (m, 1H, Ar–H), 7.96–8.00 (m, 1H, Ar–H). ^{13}C NMR (DMSO-d_6): δ 27.3 (+, CH_3), 109.7 (+, Ar–C), 115.8 (+, Ar–C), 125.5 (+, Ar–C), 126.0 (+, Ar–C), 129.5 (C_{quart}, Ar–C), 145.9 (C_{quart}, Ar–C), 170.9 (C_{quart}, CO), 178.8 (C_{quart}, CS). MS (EI): *m*/*z* (%) 193 ([M$^{\bullet+}$], 17), 151 ([M − CH_2CO]$^+$, 100). Anal. ($C_9H_7NO_2S$) C, H, N, S.

*4.1.7.2. 1-(2-Thioxobenzo[d]oxazol-3(2H)-yl)propan-1-one (**23**). Method A*: Reaction of **19** (0.50 g, 3.31 mmol) with propanoyl chloride (0.30 ml, 3.44 mmol); recrystallization from ethanol. Yield: 0.30 g (1.45 mmol, 44%, white needles). Mp: 81–82 °C. ^{1}H NMR (DMSO-d_6): δ 1.18 (t, 3H, ^3J = 7.1 Hz, CH_3), 3.43 (q, 2H, ^3J = 7.1 Hz, CH_2), 7.38–7.43 (m, 2H, Ar–H), 7.55–7.60 (m, 1H, Ar–H), 7.99–8.04 (m, 1H, Ar–H). ^{13}C NMR (DMSO-d_6): δ 8.2 (+, CH_3), 32.3 (−, CH_2), 109.7 (+, Ar–C), 115.9 (+, Ar–C), 125.3 (+, Ar–C), 126.0 (+, Ar–C), 129.7 (C_{quart}, Ar–C), 146.0 (C_{quart}, Ar–C), 174.6 (C_{quart}, CO), 179.5 (C_{quart}, CS). MS (EI): *m*/*z* (%) 207 ([M$^{\bullet+}$], 22), 179 ([M − C_2H_4]$^+$, 14), 151 ([M − CH_3CHCO]$^+$, 100). Anal. ($C_{10}H_9NO_2S$) C, H, N.

*4.1.7.3. 1-(2-Thioxobenzo[d]oxazol-3(2H)-yl)hexan-1-one (**24**). Method B*: Reaction of **19** (0.50 g, 3.31 mmol) with hexanoic anhydride (0.76 ml, 3.30 mmol); purification by chromatography on a silica gel column, elution with chloroform; analytically pure product was obtained by recrystallization from methanol. Yield: 0.30 g (1.20 mmol, 36%, white solid). Mp: 46–47.5 °C. ^{1}H NMR ($CDCl_3$): δ 0.94 (t, 3H, ^3J = 7.1 Hz, $(CH_2)_4\underline{CH_3}$), 1.32–1.48 (m, 4H, $(\underline{CH_2})_2CH_3$), 1.77–1.88 (m, 2H, $COCH_2\underline{CH_2}-$), 3.51 (t, 2H, ^3J = 7.3 Hz, $COCH_2-$), 7.27–7.35 (m, 3H, Ar–H), 8.06–8.12 (m, 1H, Ar–H). ^{13}C NMR ($CDCl_3$): δ 14.0 (+, CH_3), 22.5 (−, CH_2), 24.0 (−, CH_2), 31.1 (−, CH_2), 39.2 (−, CH_2), 109.7 (+, Ar–C), 116.5 (+, Ar–C), 125.5 (+, Ar–C), 126.1 (+, Ar–C), 130.0 (C_{quart}, Ar–C), 146.6 (C_{quart}, Ar–C), 174.3 (C_{quart}, CO), 178.8 (C_{quart}, CS). MS (EI): *m*/*z* (%) 249 ([M$^{\bullet+}$], 8), 221 ([M − CO]$^+$, 10), 151 ([M − C_4H_9CHCO]$^+$, 100). Anal. ($C_{13}H_{15}NO_2S$) C, H, N.

*4.1.7.4. 1-(2-Thioxobenzo[d]oxazol-3(2H)-yl)decan-1-one (**25**). Method A*: Reaction of **19** (0.50 g, 3.31 mmol) with decanoyl chloride (0.69 ml, 3.35 mmol); stirring for 3 h; recrystallization from methanol. Yield: 0.51 g (1.67 mmol, 51%, white solid). Mp: 64.5–65 °C. ^{1}H NMR ($CDCl_3$): δ 0.88 (t, 3H, ^3J = 6.9 Hz, $(CH_2)_8\underline{CH_3}$), 1.25–1.42 (m, 12H, $(\underline{CH_2})_6CH_3$), 1.76–1.87 (m, 2H, $COCH_2\underline{CH_2}-$), 3.51 (t, 2H, ^3J = 7.3 Hz, $COCH_2-$), 7.29–7.36 (m, 3H, Ar–H), 8.05–8.12 (m, 1H, Ar–H). ^{13}C NMR ($CDCl_3$): δ 14.1 (+, CH_3), 22.7 (−, CH_2), 24.3 (−, CH_2), 29.0 (−, CH_2), 29.3 (−, CH_2), 29.4 (−, $2CH_2$), 31.9 (−, CH_2), 39.2 (−, CH_2), 109.7 (+, Ar–C), 116.5 (+, Ar–C), 125.5 (+, Ar–C), 126.1 (+, Ar–C), 130.0 (C_{quart}, Ar–C), 146.6 (C_{quart}, Ar–C), 174.3 (C_{quart}, CO), 178.8 (C_{quart}, CS). MS (EI, 70 eV): *m*/*z* (%) 305 ([M$^{\bullet+}$], 2), 277 ([M − CO]$^+$, 2), 151 ([M − $C_8H_{17}CHCO$]$^+$, 100). Anal. ($C_{17}H_{23}NO_2S$) C, H, N, S.

*4.1.7.5. 1-(2-Thioxobenzo[d]oxazol-3(2H)-yl)hexadecan-1-one (**26**). Method A*: Reaction of **19** (0.51 g, 3.37 mmol) with hexadecanoyl chloride (1.00 ml, 3.31 mmol); stirring for 3 h; recrystallization from methanol. Yield: 0.65 g (1.67 mmol, 50%, white solid). Mp: 81–81.5 °C. ^{1}H NMR ($CDCl_3$): δ 0.88 (t, 3H, ^3J = 6.7 Hz, $(CH_2)_{14}\underline{CH_3}$), 1.23–1.50 (m, 24H, $CH_2(\underline{CH_2})_{12}CH_3$), 1.76–1.87 (m, 2H, $COCH_2\underline{CH_2}-$), 3.51 (t, 2H, ^3J = 7.3 Hz, $COCH_2-$), 7.28–7.37 (m, 3H, Ar–H), 8.05–8.11 (m, 1H, Ar–H). ^{13}C NMR ($CDCl_3$): δ 14.1 (+, CH_3), 22.7 (−, CH_2), 24.3 (−, CH_2), 28.9 (−, CH_2), 29.4 (−, $2CH_2$), 29.5 (−, CH_2), 29.6 (−, CH_2), 29.7 (−, $5CH_2$), 31.9 (−, CH_2), 39.2 (−, CH_2), 109.6 (+, Ar–C), 116.5 (+, Ar–C), 125.5 (+, Ar–C), 126.0 (+, Ar–C), 130.0 (C_{quart}, Ar–C), 146.5 (C_{quart}, Ar–C), 174.3 (C_{quart}, CO), 178.8 (C_{quart}, CS). MS (EI, 70 eV): *m*/*z* (%) 389 ([M$^{\bullet+}$], 25), 361 ([M − CO]$^+$, 83), 151 ([M − $C_{14}H_{29}CHCO$]$^+$, 100). Anal. ($C_{23}H_{35}NO_2S$) C, N. H: calcd, 9.06; found 9.54.

*4.1.7.6. 2-Phenyl-1-(2-thioxobenzo[d]oxazol-3(2H)-yl)ethanone (**27**). Method A*: Reaction of **19** (0.50 g, 3.31 mmol) with phenylacetyl

chloride (0.44 ml, 3.33 mmol) in 10 ml anhydrous acetone; recrystallization from ethanol. Yield: 0.28 g (1.04 mmol, 31%, white solid). Mp: 132.5–134 °C. ^{1}H NMR (DMSO-d_6): δ 3.56 (s, 2H, CH_2), 7.23–7.32 (m, 8H, Ar–H), 7.49–7.54 (m, 1H, Ar–H). ^{13}C NMR (DMSO-d_6): δ 40.6 (–, CH_2), 109.9 (+, Ar–C), 110.3 (+, Ar–C), 123.7 (+, Ar–C), 125.1 (+, Ar–C), 126.5 (+, Ar–C), 128.1 (+, 2Ar–C), 129.3 (+, 2Ar–C), 131.1 (C_{quart}, Ar–C), 134.9 (C_{quart}, Ar–C), 148.1 (C_{quart}, Ar–C), 172.6 (C_{quart}, CO), 178.9 (C_{quart}, CS). MS (EI): *m/z* (%) 269 ([M•$^+$], 26), 151 ([M – C_6H_5CHCO]$^+$, 28), 118 ([C_6H_5 – CHCO]$^+$, 85), 91 ([$C_6H_5CH_2$]$^+$, 100). Anal. ($C_{15}H_{11}NO_2S$) C, H, N.

*4.1.7.7. 3-Phenyl-1-(2-thioxobenzo[d]oxazol-3(2H)-yl)propan-1-one (**28**). Method A*: Reaction of **19** (0.50 g, 3.31 mmol) with 3-phenylpropionyl chloride (0.66 g, 3.91 mmol); recrystallization from ethanol. Yield: 0.33 g (1.16 mmol, 35%, yellow solid). Mp: 73–75 °C. ^{1}H NMR (DMSO-d_6): δ 3.06 (t, 2H, ^3J = 7.4 Hz, $COCH_2CH_2Ph$), 3.87 (t, 2H, ^3J = 7.4 Hz, $COCH_2CH_2Ph$), 7.16–7.26 (m, 4H, Ar–H), 7.39–7.44 (m, 2H, Ar–H), 7.56–7.61 (m, 1H, Ar–H), 7.74–7.79 (m, 1H, Ar–H), 7.98–8.03 (m, 1H, Ar–H). ^{13}C NMR (DMSO-d_6): δ 29.5 (–, CH_2), 40.1 (–, CH_2), 109.8 (+, Ar–C), 110.9 (+, Ar–C), 115.8 (+, Ar–C), 119.5 (+, Ar–C), 125.2 (+, Ar–C), 125.5 (+, Ar–C), 125.9 (+, Ar–C), 128.2 (+, 2Ar–C), 129.6 (C_{quart}, Ar–C), 140.1 (C_{quart}, Ar–C), 146.0 (C_{quart}, Ar–C), 173.1 (C_{quart}, CO), 179.3 (C_{quart}, CS). MS (EI): *m/z* (%) 283 ([M•$^+$], 15), 250 ([M – SH]$^+$, 64), 151 ([M – $C_6H_5CH_2CHCO$]$^+$, 100), 105 ([$C_6H_5CH_2CH_2$]$^+$, 69), 91 ([$C_6H_5CH_2$]$^+$, 78). Anal. ($C_{16}H_{13}NO_2S$) C, H, N.

*4.1.7.8. 4-Phenyl-1-(2-thioxobenzo[d]oxazol-3(2H)-yl)butan-1-one (**29**). Method A*: Reaction of **19** (0.50 g, 3.31 mmol) with 4-phenylbutanoyl chloride (0.87 g, 4.76 mmol); the reaction mixture was extracted two times with chloroform (15 ml); the combined organic phases were dried over magnesium sulfate and the solvent was removed under reduced pressure; purification by column chromatography on silica gel, elution with chloroform. Yield: 0.13 g (0.44 mmol, 13%, brown solid). Mp: 145–146.5 °C. ^{1}H NMR (DMSO-d_6): δ 1.71–1.89 (m, 2H, $COCH_2CH_2CH_2Ph$), 2.21 (t, 2H, ^3J = 7.4 Hz, $COCH_2$–), 2.56 (t, 2H, ^3J = 7.4 Hz, $CO(CH_2)_2CH_2Ph$), 7.14–7.20 (m, 3H, Ar–H), 7.21–7.34 (m, 5H, Ar–H), 7.42–7.60 (m, 1H, Ar–H). ^{13}C NMR (DMSO-d_6): δ 26.2 (–, CH_2), 32.9 (–, CH_2), 34.3 (–, CH_2), 109.9 (+, Ar–C), 110.4 (+, Ar–C), 123.7 (+, Ar–C), 125.1 (+, Ar–C), 125.7 (+, Ar–C), 128.2 (+, Ar–C), 128.2 (+, 3Ar–C), 131.1 (C_{quart}, Ar–C), 141.4 (C_{quart}, Ar–C), 148.0 (C_{quart}, Ar–C), 174.2 (C_{quart}, CO), 180.0 (C_{quart}, CS). MS (EI): *m/z* (%) 264 ([M – SH]$^+$, 55), 151 ([M – $C_6H_5(CH_2)_2CHCO$]$^+$, 58), 147 ([$C_6H_5CH_2CH_2CH_2CO$]$^+$, 65), 91 ([$C_6H_5CH_2$]$^+$, 100). Anal. ($C_{17}H_{15}NO_2S$) C, H, N.

*4.1.7.9. (E)-3-Phenyl-1-(2-thioxobenzo[d]oxazol-3(2H)-yl)prop-2-en-1-one (**30**). Method A*: Reaction of **19** (0.50 g, 3.31 mmol) with cinnamoyl chloride (0.55 g, 3.30 mmol); recrystallization from ethanol. Yield: 0.53 g (1.88 mmol, 57%, yellow powder). Mp: 150.5–151.5 °C (Mp: 148–149 °C [47]). ^{1}H NMR (DMSO-d_6): δ 7.41–7.46 (m, 2H, Ar–H), 7.49–7.53 (m, 3H, Ar–H), 7.61–7.66 (m, 1H, Ar–H), 7.73–7.81 (m, 2H, Ar–H), 7.83–7.89 (m, 1H, Ar–H), 7.93 (d, 1H, ^3J = 15.8 Hz, =CH), 8.04 (d, 1H, ^3J = 15.8 Hz, =CH). ^{13}C NMR (DMSO-d_6): δ 110.1 (+, Ar–C), 114.6 (+, Ar–C), 119.7 (+, =CH), 125.6 (+, Ar–C), 126.0 (+, Ar–C), 128.7 (+, Ar–C), 129.2 (+, 3Ar–C), 129.6 (C_{quart}, Ar–C), 131.2 (+, Ar–C), 134.0 (C_{quart}, Ar–C), 145.8 (+, =CH), 146.5 (C_{quart}, Ar–C), 165.5 (C_{quart}, CO), 178.4 (C_{quart}, CS). MS (EI): *m/z* (%) 281 ([M•$^+$], 16), 253 ([M – CO]$^+$, 3), 151 ([M – $C_6H_5CHCHCO$]$^+$, 9), 131 ([$C_6H_5CHCHCO$]$^+$, 100), 103 ([C_6H_5–CH=CH]$^+$, 34), 77 ([C_6H_5]$^+$, 18). Anal. ($C_{16}H_{11}NO_2S$) C, H, N.

*4.1.7.10. 3-Cyclohexyl-1-(2-thioxobenzo[d]oxazol-3(2H)-yl)propan-1-one (**31**). Method A*: Reaction of **19** (0.5 g, 3.31 mmol) with 3-cyclohexylpropanoyl chloride (0.80 g, 4.58 mmol); recrystallization from ethanol. Yield: 0.54 g (1.87 mmol, 56%, white solid). Mp: 76–77.5 °C. ^{1}H NMR ($CDCl_3$): δ 0.89–1.44 (m, 5H, $2CH_2CH$), 1.62–1.83 (m, 8H, $4CH_2$), 3.53 (t, 2H, ^3J = 7.7 Hz, $COCH_2$–), 7.27–7.36 (m, 3H, Ar–H), 8.05–8.10 (m, 1H, Ar–H). ^{13}C NMR ($CDCl_3$): δ 26.2 (–, $2CH_2$), 26.5 (–, CH_2), 31.6 (–, CH_2), 33.1 (–, $2CH_2$), 36.9 (–, CH_2), 37.1 (+, CH), 109.6 (+, Ar–C), 116.5 (+, Ar–C), 125.5 (+, Ar–C), 126.0 (+, Ar–C), 130.0 (C_{quart}, Ar–C), 146.5 (C_{quart}, Ar–C), 174.6 (C_{quart}, CO), 178.8 (C_{quart}, CS). MS (EI): *m/z* (%) 289 ([M•$^+$], 5), 151 ([M – $C_6H_{11}CH_2CHCO$]$^+$, 100), 121 (benzoxazole, 56). Anal. ($C_{16}H_{19}NO_2S$) H, N. C: calcd, 66.40; found 65.86.

*4.1.7.11. 2-Phenoxy-1-(2-thioxobenzo[d]oxazol-3(2H)-yl)ethanone (**32**). Method A*: Reaction of **19** (0.50 g, 3.31 mmol) with phenoxyacetyl chloride (0.46 ml, 3.33 mmol); recrystallization from ethanol. Yield: 0.32 g (1.12 mmol, 34%, light-brown solid). Mp: 138–139 °C. ^{1}H NMR (DMSO-d_6): δ 4.66 (s, 2H, CH_2), 6.84–6.99 (m, 3H, Ar–H), 7.21–7.33 (m, 2H, Ar–H), 7.36–7.53 (m, 2H, Ar–H), 7.77 (d, 2H, ^3J = 6.8 Hz, Ar–H). ^{13}C NMR (DMSO-d_6): δ 64.2 (–, CH_2), 110.9 (+, Ar–C), 114.3 (+, 2Ar–C), 119.5 (+, Ar–C), 120.8 (+, Ar–C), 125.2 (+, Ar–C), 125.9 (+, Ar–C), 129.3 (+, 2Ar–C), 141.1 (C_{quart}, Ar–C), 151.7 (C_{quart}, Ar–C), 157.6 (C_{quart}, Ar–C), 160.0 (C_{quart}, CO), 170.1 (C_{quart}, CS). MS (EI): *m/z* (%) 285 ([M•$^+$], 36), 192 ([M – OC_6H_5]$^+$, 46), 164 ([M – OC_6H_5CO]$^+$, 100), 151 ([M – C_6H_5OCHCO]$^+$, 34), 77 ([C_6H_5]$^+$, 71). Anal. ($C_{15}H_{11}NO_3S$) C, H, N.

*4.1.7.12. Benzyl 2-thioxobenzo[d]oxazol-3(2H)-carboxylate (**33**). Method A*: Reaction of **19** (0.50 g, 3.31 mmol) with benzyl chloroformate (0.48 ml, 3.36 mmol); different workup: reaction mixture was concentrated under reduced pressure and ethyl acetate (15 ml) and water (10 ml) were added; the organic phase was dried over magnesium sulfate and the solvent was removed under reduced pressure; crystallization from petroleum ether (60–80 °C) and subsequent recrystallization from methanol. Yield: 0.30 g (1.05 mmol, 32%, white needles). Mp: 86–87 °C (Mp: 89–92 °C [48]). ^{1}H NMR (DMSO-d_6): δ 5.55 (s, 2H, CH_2), 7.31–7.51 (m, 5H, Ar–H), 7.52–7.62 (m, 3H, Ar–H), 7.66–7.73 (m 1H, Ar–H). ^{13}C NMR (DMSO-d_6): δ 69.7 (–, CH_2), 110.0 (+, Ar–C), 115.0 (+, Ar–C), 125.3 (+, Ar–C), 125.9 (+, 2Ar–C), 128.6 (+, 4Ar–C), 128.8 (C_{quart}, Ar–C), 134.3 (C_{quart}, Ar–C), 145.6 (C_{quart}, Ar–C), 148.8 (C_{quart}, CO), 176.4 (C_{quart}, CS). MS (EI): *m/z* (%) 285 ([M•$^+$], 5), 91 ([$C_6H_5CH_2$]$^+$, 100). Anal. ($C_{15}H_{11}NO_3S$) C, H, N.

*4.1.7.13. Methyl-3-(3-phenylpropanoyl)-2,3-dihydro-2-thioxobenzo[d]oxazole-5-carboxylate (**34**)*

*4.1.7.13.1. Synthesis of methyl 2-sulfanylbenzo[d]oxazole-5-carboxylate (**21**).* 3-Amino-4-hydroxybenzoic acid (0.40 g, 2.61 mmol) was dissolved in anhydrous methanol (10 ml) and treated with TMSCl (0.75 ml, 5.94 mmol). The mixture was stirred at 55 °C for 2 days. After evaporation of the solvent, the obtained residue was purified by column chromatography on silica gel eluting with ethyl acetate (yield: 0.25 g, 1.50 mmol, 57%, white solid). 0.20 g of the obtained methyl 3-amino-4-hydroxybenzoate, dissolved in anhydrous THF (10 ml), was mixed with TCDI (0.26 g, 1.46 mmol) under an inert atmosphere. The solution was stirred overnight at room temperature. After evaporation of the solvent the residue was treated with water (15 ml) and extracted with ethyl acetate (3 × 15 ml). The combined organic layers were dried over magnesium sulfate and concentrated under reduced pressure. The remaining crude product was recrystallized from ethanol yielding 0.22 g (1.05 mmol, 88%) of methyl 2-sulfanylbenzo[*d*]oxazole-5-carboxylate (**21**) as a brown solid. Mp: 203–205 °C.

Method A: Reaction of methyl 2-sulfanylbenzo[*d*]oxazole-5-carboxylate (**21**) (0.20 g, 0.96 mmol) with 3-phenylpropanoyl chloride (0.15 ml, 0.96 mmol); recrystallization from ethanol. Yield: 0.17 g (0.50 mmol, 52%, beige solid). Mp: 112.5–115.5 °C. ^{1}H

NMR ($CDCl_3$): δ 3.17 (t, 2H, ^3J = 7.5 Hz, $COCH_2CH_2Ph$), 3.85 (t, 2H, ^3J = 7.5 Hz, $COCH_2CH_2Ph$), 3.95 (s, 3H, CO_2CH_3), 7.22–7.36 (m, 6H, Ar–H), 8.09 (dd, 1H, ^3J = 8.5 Hz, ^4J = 1.7 Hz, H-6), 8.74 (dd, 1H, ^4J = 1.7 Hz, ^5J = 0.6 Hz, H-4). ^{13}C NMR ($CDCl_3$): δ 30.1 (–, CH_2), 40.7 (–, CH_2), 52.6 (+, CH_3), 109.4 (+, Ar–C), 117.9 (+, Ar–C), 126.5 (+, Ar–C), 127.9 (C_{quart}, Ar–C), 128.4 (+, Ar–C), 128.5 (+, 2Ar–C), 128.7 (+, 2Ar–C), 130.1 (C_{quart}, Ar–C), 139.7 (C_{quart}, Ar–C), 149.4 (C_{quart}, Ar–C), 165.9 (C_{quart}, CO_2Me), 173.0 (C_{quart}, CO), 178.6 (C_{quart}, CS). MS (EI): *m/z* (%) 341 ([M$^{\bullet+}$], 8), 308 ([M – SH]$^+$, 36), 209 ([M – $C_6H_5CH_2CHCO$]$^+$, 87), 178 ([M – $C_6H_5CH_2CHCOOCH_3$]$^+$, 35), 105 ([$C_6H_5CH_2CH_2$]$^+$, 100), 91 ([$C_6H_5CH_2$]$^+$, 89). Anal. ($C_{18}H_{15}NO_4S$) C, H, N.

4.1.8. 3-Acetylbenzo[d]oxazol-2(3H)-one (**35**)

The protocol described in Ref. [31] was modified. Benzoxazol-2-one (**20**) (0.67 g, 4.96 mmol), dissolved in anhydrous THF (10 ml), and triethylamine (2.0 ml, 14.43 mmol) were mixed under a nitrogen atmosphere. After cooling in an ice bath, acetyl chloride (0.43 ml, 6.03 mmol) was added dropwise. The reaction mixture was heated under reflux for 2 h and then poured into ice-cold water (100 ml). After stirring for 1 h, the precipitate was collected, washed with water and recrystallized from ethanol. Yield: 0.28 g (1.58 mmol, 32%, white solid). Mp: 90.5–91.5 °C (Mp: 95–96 °C [31]). ^{1}H NMR (DMSO-d_6): δ 2.61 (s, 3H, $COCH_3$), 7.22–7.37 (m, 2H, Ar–H), 7.38–7.48 (m, 1H, Ar–H), 7.89–7.99 (m, 1H, Ar–H). ^{13}C NMR ($CDCl_3$): δ 24.6 (+, CH_3), 109.7 (+, Ar–C), 115.0 (+, Ar–C), 124.4 (+, Ar–C), 124.9 (+, Ar–C), 127.7 (C_{quart}, Ar–C), 141.7 (C_{quart}, Ar–C), 150.9 (C_{quart}, CO), 169.6 (C_{quart}, CO). MS (EI): *m/z* (%) 177 ([M$^{\bullet+}$], 26), 135 ([M – CH_2CO]$^+$, 100), 43 ([CH_3CO]$^+$, 84). Anal. ($C_9H_7NO_3$) C, H, N.

4.1.9. 3-Hexanoylbenzo[d]oxazol-2(3H)-one (**36**)

The protocol described in Ref. [31] was modified. Benzoxazol-2-one (**20**) (0.50 g, 3.70 mmol) was dissolved in dry THF (10 ml) under an inert atmosphere, triethylamine (0.63 ml, 4.54 mmol) and hexanoic anhydride (1.03 ml, 4.47 mmol) were added, and the mixture was heated under reflux for 4 h. Then water (15 ml) was added and the mixture was extracted three times with ethyl acetate (15 ml). The combined organic layers were washed with a saturated solution of sodium carbonate (15 ml), dried over magnesium sulfate and concentrated *in vacuo*. The crude product was purified by column chromatography on silica gel eluting with chloroform. Yield: 0.60 g (2.57 mmol, 70%, pale light-brown solid). Mp: 72.5–73.5 °C. ^{1}H NMR (DMSO-d_6): δ 0.80–0.99 (m, 3H, CH_3), 1.24–1.43 (m, 4H, $(CH_2)_2CH_3$), 1.60–1.71 (m, 2H, $COCH_2CH_2$–), 3.02 (t, 2H, ^3J = 7.4 Hz, $COCH_2$–), 7.23–7.34 (m, 2H, Ar–H), 7.36–7.50 (m, 1H, Ar–H), 7.89–8.05 (m, 1H, Ar–H). ^{13}C NMR (DMSO-d_6): δ 13.7 (+, CH_3), 21.8 (–, CH_2), 22.8 (–, $COCH_2CH_2$), 30.5 (–, $CO(CH_2)_2CH_2$), 35.7 (–, $COCH_2$–), 109.7 (+, Ar–C), 115.1 (+, Ar–C), 124.3 (+, Ar–C), 124.8 (+, Ar–C), 127.8 (C_{quart}, Ar–C), 141.8 (C_{quart}, Ar–C), 150.8 (C_{quart}, CO), 172.4 (C_{quart}, CO). MS (EI): *m/z* (%) 233 ([M$^{\bullet+}$], 29), 135 ([M – C_4H_9CHCO]$^+$, 100), 99 ([C_4H_9CHCO]$^+$, 60), 71 ([C_4H_9 – CH_2]$^+$, 44). Anal. ($C_{13}H_{15}NO_3$) C, H, N.

4.1.10. 3-Ethylbenzo[d]oxazole-2(3H)-thione (**38**)

The protocol described in Ref. [36] was modified. 2-(Ethylamino) phenol (**37**) [34] (0.15 g, 1.09 mmol) was dissolved in dry THF (5 ml) under an inert atmosphere. Subsequently, TCDI (0.21 g, 1.20 mmol) was added in small portions and the mixture was stirred for 3 h at ambient temperature. The reaction mixture was concentrated under reduced pressure, and water (15 ml) was added. After extraction with ethyl acetate (3 × 15 ml), the combined organic layers were dried over magnesium sulfate and evaporated *in vacuo*. The crude product was purified by column chromatography on silica gel eluting with a 3:1 (v/v) mixture of petroleum ether (60–80 °C) and ethyl acetate. Yield: 0.07 g (0.39 mmol, 36%, beige solid). Mp: 105–107 °C (Mp. 96–98 °C [36]). ^{1}H NMR (DMSO-d_6): δ 1.30 (t, 3H, ^3J = 7.2 Hz, CH_3), 4.24 (q, 2H, ^3J = 7.2 Hz, CH_2), 7.30–7.43 (m, 2H, Ar–H), 7.48–7.63 (m, 2H, Ar–H). ^{13}C NMR ($CDCl_3$): δ 11.7 (+, CH_3), 40.2 (–, CH_2), 110.1 (+, Ar–C), 110.5 (+, Ar–C), 124.3 (+, Ar–C), 125.1 (+, Ar–C), 131.0 (C_{quart}, Ar–C), 146.4 (C_{quart}, Ar–C), 178.6 (C_{quart}, CS). MS (EI): *m/z* (%) 179 ([M$^{\bullet+}$], 100), 151 ([M – C_2H_4]$^+$, 93). Anal. (C_9H_9NOS) C, H, N.

4.2. Hyaluronan lyase assay

Hyaluronan (hyaluronic acid) from *Streptococcus zooepidemicus* was purchased from Aqua Biochem (Dessau, Germany). Bovine serum albumin (BSA) was obtained from Serva (Heidelberg, Germany). Stabilized hyaluronan lyase, i.e., 200,000 units (0.572 mg from *S. agalactiae* strain 4755 plus 2.2 mg of BSA and 37 mg of Tris–HCl per vial) of lyophilized *Sag*Hyal$_{4755}$, was kindly provided by id-Pharma (Jena, Germany). All other chemicals were of analytical grade and were received from Merck or Sigma.

To determine the solubility of the inhibitors, a sample containing 600 µl of citrate–phosphate buffer (pH 5 and pH 7.4), 396 µl of water, 300 µl of BSA solution (0.2 mg/ml in water) and a solution of 54 µl of the respective test compound (dissolved in DMSO) of various concentrations was measured at 600 nm. A cuvette filled with water served as reference. Compounds were tested for hyaluronan lyase inhibition at concentrations, where no turbidity was measured.

The inhibitory effects of the compounds on *Sag*Hyal$_{4755}$ were measured using a turbidimetric assay [37]. Enzyme activity was quantified by determining the turbidity caused by the residual high molecular weight substrate (molecular weight > 6–8 kDa) precipitated with cetyltrimethylammonium bromide (CTAB). The incubation mixture contained 120 µl of citrate–phosphate buffer (solution A: 0.1 M Na_2HPO_4/0.1 M NaCl, solution B: 0.1 M citric acid/0.1 M NaCl, solution A and B were mixed in appropriate proportions to reach pH 5.0 and 7.4, respectively), 30 µl of BSA solution (0.2 mg/ml in water), 30 µl of HA substrate solution (2 mg/ml in water), 50 µl H_2O, 10 µl dimethyl sulfoxide (DMSO) and 30 µl enzyme solution (2.9 ng of *Sag*Hyal$_{4755}$ in 30 µl BSA solution). To determine the enzyme activities in the presence of the test compounds, instead of 10 µl DMSO, 10 µl of varying concentrations of inhibitors were used. The final DMSO concentration was 3.8% (v/v).

After incubation of the assay mixture for 30 min (pH 5) or for 3 h (pH 7.4) at 37 °C, 720 µl of a 2.5% (m/v) cetyltrimethylammonium bromide solution (2.5 g CTAB dissolved in 100 ml 0.5 M sodium hydroxide solution, pH 12.5) were added to precipitate the residual high molecular weight substrate and to stop the enzyme reaction. This mixture was again incubated at 25 °C for 20 min, and the turbidity of each sample was determined at 600 nm with an Uvikon 930 UV spectrophotometer (Kontron, Eching, Germany).

The turbidity of the sample without inhibitor was taken as reference for 100% enzyme activity, whereas the turbidity of the sample without enzyme (30 µl BSA) was taken as reference for 0% enzyme activity. The activities were plotted against the logarithm of the inhibitor concentration. $IC_{50} \pm$ SEM values were calculated by curve fitting of the experimental data with Sigma Plot 8.0 (SPSS Inc., Chicago, IL) and are the means of at least two independent experiments performed in duplicate. To exclude factors affecting turbidity (interactions of the test compound with the substrate, absorption by the test compound etc.), controls containing the incubation mixture without enzyme (30 µl of BSA solution was used instead) were run in parallel.

4.3. Molecular models of SpnHyal in complex with ligands

The *Spn*Hyal crystal structures PDB ID 1EGU [12] (free), 2BRP [16] (cpd. **5**), 1LOH [11] (hexasaccharide) and 1W3Y [15] (Vcpal) were taken from the Brookhaven Protein Databank [52]. Modeling

approaches were performed using the BIOPOLYMER module of the software package SYBYL 7.3 (Tripos, L.P., St. Louis, USA). Energy minimizations were based on the AMBER FF99 force field [53] with AMBER FF99 charges (distance dependent dielectric constant of 4) up to a root mean square gradient of 0.05 kcal/mol/Å (Powell conjugate gradient method). Surfaces and lipophilic potentials (protein variant with the new Crippen parameter table [54,55]) of the model were calculated and visualized by the program MOLCAD (MOLCAD GmbH, Darmstadt, Germany) contained within SYBYL.

Acknowledgment

This study was supported by the Graduate Research Training Program of the Deutsche Forschungsgemeinschaft (Graduiertenkolleg 760 “Medicinal Chemistry”), by the Bayerische Forschungsstiftung (AZ-829-08) and by the Studienstiftung des Deutschen Volkes (A.Bo.).

References

[1] K. Meyer, J.W. Palmer, The polysaccharide of the vitreous humor, J. Biol. Chem. 107 (1934) 629–634.
[2] T. Laurent, J. Fraser, Hyaluronan, FASEB J. 6 (1992) 2397–2405.
[3] A.J. Day, G.D. Prestwich, Hyaluronan-binding proteins: tying up the giant, J. Biol. Chem. 277 (2002) 4585–4588.
[4] T.C. Laurent, U.B. Laurent, J.R. Fraser, The structure and function of hyaluronan: an overview, Immunol. Cell Biol. 74 (1996) A1–A7.
[5] T. Csoka, G. Frost, R. Stern, Hyaluronidases in tissue invasion, Inv. Metastasis 17 (1997) 297–311.
[6] G. Kreil, Hyaluronidases - a group of neglected enzymes, Prot. Sci. 4 (1995) 1666–1669.
[7] B.L. Cantarel, P.M. Coutinho, C. Rancurel, T. Bernard, V. Lombard, B. Henrissat, The carbohydrate-active enzymes database (CAZy): an expert resource for glycogenomics, Nucleic Acids Res. 37 (2009) D233–D238.http://www.cazy.org/.
[8] A. Linker, K. Meyer, Production of unsaturated uronides by bacterial hyaluronidases, Nature 174 (1954) 1192–1194.
[9] M. Jedrzejas, L. Chantalat, Structural studies of *Streptococcus agalactiae* hyaluronate lyase, Acta Crystallograph. D 56 (2000) 460–463.
[10] M.J. Jedrzejas, Three-dimensional structures of hyaluronate lyases from Streptococcus species and their mechanism of hyaluronan degradation, in: science of hyaluronan today, Glycoforum (2002).www.glycoforum.gr.jp.
[11] M.J. Jedrzejas, L.V. Mello, B.L. De Groot, S. Li, Mechanism of hyaluronan degradation by *Streptococcus pneumoniae* hyaluronate lyase: structures of complexes with the substrate, J. Biol. Chem. 277 (2002) 28287–28297.
[12] S. Li, S. Kelly, E. Lamani, M. Ferraroni, M. Jedrzejas, Structural basis of hyaluronan degradation by *Streptococcus pneumoniae* hyaluronate lyase, EMBO J. 19 (2000) 1228–1240.
[13] S. Li, M.J. Jedrzejas, Hyaluronan binding and degradation by *Streptococcus agalactiae* hyaluronate lyase, J. Biol. Chem. 276 (2001) 41407–41416.
[14] S. Li, K.B. Taylor, S.J. Kelly, M.J. Jedrzejas, Vitamin C inhibits the enzymatic activity of *Streptococcus pneumoniae* hyaluronate lyase, J. Biol. Chem. 276 (2001) 15125–15130.
[15] A. Botzki, D.J. Rigden, S. Braun, M. Nukui, S. Salmen, J. Hoechstetter, G. Bernhardt, S. Dove, M.J. Jedrzejas, A. Buschauer, L-Ascorbic acid 6-hexadecanoate, a potent hyaluronidase inhibitor. X-ray structure and molecular modeling of enzyme-inhibitor complexes, J. Biol. Chem. 279 (2004) 45990–45997.
[16] D.J. Rigden, A. Botzki, M. Nukui, R.B. Mewbourne, E. Lamani, S. Braun, E. von Angerer, G. Bernhardt, S. Dove, A. Buschauer, M.J. Jedrzejas, Design of new benzoxazole-2-thione derived inhibitors of *Streptococcus pneumoniae* hyaluronan lyase: structure of a complex with a 2-phenylindole, Glycobiology 16 (2006) 757–765.
[17] K. Ponnuraj, M. Jedrzejas, Mechanism of hyaluronan binding and degradation: structure of *Streptococcus pneumoniae* haluronate lyase in complex with hyaluronic acid disaccharide at 1.7 Å resolution, J. Mol. Biol. 299 (2000) 885–895.
[18] W. Hynes, S. Walton, Hyaluronidases of gram-positive bacteria, FEMS Microbiol. Lett. 183 (2000) 201–207.
[19] K.S. Girish, K. Kemparaju, S. Nagaraju, B.S. Vishwanath, Hyaluronidase inhibitors: a biological and therapeutic perspective, Curr. Med. Chem. 16 (2009) 2261–2288.
[20] K. Suzuki, Y. Terasaki, M. Uyeda, Inhibition of hyaluronidases and chondroitinases by fatty acids, J. Enzym. Inhib. Med. Chem. 17 (2002) 183–186.
[21] W. Hertel, G. Peschel, J.H. Ozegowski, P.J. Willer, Inhibitory effects of triterpenes and flavonoids on the enzymatic activity of hyaluronic acid-splitting enzymes, Arch. Pharm. 339 (2006) 313–318.
[22] E. Klein, N. Weber, in vitro test for the effectiveness of antioxidants as inhibitors of thiyl radical-induced reactions with unsaturated fatty acids, J. Agric. Food Chem. 49 (2001) 1224–1227.
[23] A. Mitra, S. Govindwar, P. Joseph, A. Kulkarni, Inhibition of human term placental and fetal liver glutathione-S-transferases by fatty acids and fatty acid esters, Toxicol. Lett. 60 (1992) 281–288.
[24] M. Spickenreither, S. Braun, G. Bernhardt, S. Dove, A. Buschauer, Novel 6-O-acylated vitamin C derivatives as hyaluronidase inhibitors with selectivity for bacterial lyases, Bioorg. Med. Chem. Lett. 16 (2006) 5313–5316.
[25] H.J. Böhm, The computer program LUDI: a new method for the de novo design of enzyme inhibitors, J. Comput. Aided Mol. Des 6 (1992) 61–78.
[26] A. Botzki, S. Salmen, G. Bernhardt, A. Buschauer, S. Dove, Structure-Based design of bacterial hyaluronan lyase inhibitors, QSAR Comb. Sci. 24 (2005) 458–469.
[27] S. Salmen, Inhibitors of Bacterial and Mammalian Hyaluronidases: Synthesis and Structure-Activity Relationships. University of Regensburg, Regensburg, 2003.
[28] G. Walter, R. Liebl, E. von Angerer, 2-phenylindole sulfamates: inhibitors of steroid sulfatase with antiproliferative activity in MCF-7 breast cancer cells, J. Steroid Biochem. Mol. Biol. 88 (2004) 409–420.
[29] O. Algul, A. Kaessler, Y. Apcin, A. Yilmaz, J. Jose, Comparative studies on conventional and microwave synthesis of some benzimidazole, benzothiazole and indole derivatives and testing on inhibition of hyaluronidase, Molecules 13 (2008) 736–748.
[30] B.D. Saxena, R.K. Khajuria, O.P. Suri, Synthesis and spectral studies of 2-mercaptobenzimidazole derivatives, J. Heterocycl. Chem. 19 (1982) 681–683.
[31] H. Ucar, K. Van Derpoorten, P. Depovere, D. Lesieur, M. Isa, B. Masereel, J. Delarge, J.H. Poupaert, “Fries like” rearrangement: a novel and efficient method for the synthesis of 6-acyl-2(3*H*)-benzoxazolones and 6-acyl-2(3*H*)-benzothiazolones, Tetrahedron 54 (1998) 1763–1772.
[32] I.H. Chung, K.S. Cha, J.H. Seo, J.H. Kim, B.Y. Chung, C.S. Kim, 1,3-Dihydro-1,3-diacetyl-2*H*-benzimidazol-2-one: a new versatile and selective acetylating agent, Heterocycles 53 (2000) 529–533.
[33] D. Harrison, A.C.B. Smith, Acyl derivatives of 2-oxobenzimidazoline, J. Chem. Soc. (1961) 4827–4830.
[34] B. Raju, N. Nguyen, G.W. Holland, Solution-phase parallel synthesis of substituted benzimidazoles, J. Comb. Chem. 4 (2002) 320–328.
[35] M. Ueda, K. Seki, Y. Imai, S-Acyl and N-acyl derivatives of 2-mercaptobenzoxazole - new, highly reactive acylating agents for synthesis of amides and esters, Synthesis-Stuttgart (1981) 991–993.
[36] K. Giyasov, N.A. Aliev, Synthesis of N-alkylbenzoxazolinethiones, Uzbekskii Khimicheskii Zhurnal (1987) 39–40.
[37] N. Di Ferrante, Turbidimetric measurement of acid mucopolysaccharides and hyaluronidase activity, J. Biol. Chem. 220 (1956) 303–306.
[38] D.R. Doerge, N.M. Cooray, Synthesis of N-Substituted benzimidazole-2-thiones, Synth. Commun. 21 (1991) 1789–1795.
[39] M.R. Ibrahim, A.A. Jarrar, S.S. Sabri, Conformations of monoacyl and 1,3-diacylbenzimidazoline-2-thiones and dihydrobenzimidazoles, J. Heterocycl. Chem. 12 (1975) 11–13.
[40] F. Tittelbach, D. Martin, Cleavage of 1,2,4-thiadiazol-3-ones by triphenylphosphine: triphenylphosphoniothioimidazolates and their consecutive reactions, J. fuer Praktische Chem. (Leipzig) 330 (1988) 338–348.
[41] K. Sasse, F. Grewe, Fungicidal benzimidazoles, S. African (1968) ZA 6705057 19680123.
[42] R. Lok, R.E. Leone, A.J. Williams, Facile rearrangements of alkynylamino heterocycles with noble metal cations, J. Org. Chem. 61 (1996) 3289–3297.
[43] R.S. Varma, A. Kapoor, Potential biologically-active agents. 20. Synthesis of 5-carbomethoxy-3-arylaminomethylbenzoxazolin-2-thiones and related products, Pharmazie 34 (1979) 387–389.
[44] T. Nishio, K. Shiwa, Acylation and alkoxycarbonylation of benzoxazoline-2-thione and benzothiazoline-2-thione, Heterocycles 62 (2004) 313–324.
[45] I. Chiarotto, M. Feroci, M. Orsini, G. Sotgiu, A. Inesi, Electrogenerated N-heterocyclic carbenes: N-functionalization of benzoxazolones, Tetrahedron 65 (2009) 3704–3710.
[46] S.Y. Yu, H. Seino, M. Ueda, Synthesis of ordered polymer by direct polycondensation. 9. Ordered poly(amide-acylhydrazide-amide) from three nonsymmetric monomers, Macromolecules 32 (1999) 1027–1035.
[47] G.I. Uzokov, S. Masharipov, S.S. Kasymova, N.A. Aliev, N.S. Mukhamedov, Synthesis of some unsaturated 3-acylbenzoxazolinones and 3-acylbenzoxazolinethiones, Dokl. Akad. Nauk USSR (1988) 41–43.
[48] S. Romani, L. Moroder, G. Bovermann, E. Wunsch, On the use of 5-membered heterocycles in peptide chemistry, Synthesis-Stuttgart (1985) 738–742.
[49] A. Lespagnol, J. Mercier, C. Lespagnol, Benzoxazolinone and some derivatives, Arch. Int. Pharmacodyn. Ther. 94 (1953) 211–224.
[50] D.J. Fry, J.D. Kendall, Formation and fission of quaternary salts of heterocyclic bases containing reactive alkylmercapto groups, J. Chem. Soc. (1951) 1716–1722.
[51] D.J. Rigden, J.E. Littlejohn, H.V. Joshi, B.L. de Groot, M.J. Jedrzejas, Alternate structural conformations of *Streptococcus pneumoniae* hyaluronan lyase: insights into enzyme flexibility and underlying molecular mechanism of action, J. Mol. Biol. 358 (2006) 1165–1178.
[52] H.M. Berman, J. Westbrook, Z. Feng, G. Gilliland, T.N. Bhat, H. Weissig, I.N. Shindyalov, P.E. Bourne, The protein data bank, Nucleic Acids Res. 28 (2000) 235–242.
[53] W.D. Cornell, P. Cieplak, C.I. Bayly, I.R. Gould, K.M. Merz Jr., D.M. Ferguson, D.C. Spellmeyer, T. Fox, J.W. Caldwell, P.A. Kollman, A second generation force field for the simulation of proteins, nucleic acids, and organic molecules, J. Am. Chem. Soc. 117 (1995) 5179–5197.
[54] A.K. Ghose, V.N. Viswanadhan, J.J. Wendoloski, Prediction of hydrophobic (lipophilic) properties of small organic molecules using fragmental methods: an analysis of ALOGP and CLOGP methods, J. Phys. Chem. 102 (1998) 3762–3772.
[55] W. Heiden, G. Moeckel, J. Brickmann, A new approach to analysis and display of local lipophilicity/hydrophilicity mapped on molecular surfaces, J. Comput. Aided Mol. Des. 7 (1993) 503–514.